European Journal of Agronomy 170 (2025) 127728

Contents lists available at ScienceDirect

European Journal of Agronomy

journal homepage: www.elsevier.com/locate/eja

Nitrogen fertilization strategy for Swiss winter wheat under climate-induced rainfall reduction: A model-based assessment

Paola de F. Bongiovani [a,b,*], Juan Manuel Herrera [a], Emmanuel Frossard [b], Rogério de S. Nóia Júnior [c], Diego N.L. Pequeno [d], Amanda Burton [a], Lilia Levy Häner [a], Senthold Asseng [c]

[a] Agroscope, Plant Production Systems, Route de Duillier 60, Nyon 1260, Switzerland
[b] ETH Zurich, Institute of Agricultural Sciences, Group of Plant Nutrition, Lindau, Switzerland
[c] Technical University of Munich, Department of Life Science Engineering, Digital Agriculture, HEF World Agricultural Systems Center, Freising, Germany
[d] International Maize and Wheat Improvement Center (CIMMYT), Texcoco 56237, Mexico

A R T I C L E I N F O

Keywords:
Triticum aestivum
Crop model
DSSAT
Climate change
Fertilizer use
Plant nutrition
Sustainable agriculture
Nitrogen management

A B S T R A C T

Reduced rainfall and nitrogen (N) use in warm-summer humid continental climates may lower wheat yields. Our study employs the DSSAT-Nwheat process-based crop simulation model to quantify the effects of N input and rainfall on various phenological stages of the Swiss wheat genotype CH Nara, calibrated and evaluated using field data from 2018 to 2022. Simulations over 42 years (1981–2022) across five different Cambisols used historical daily weather data to test rainfall reductions from 20 % to 100 % during three critical periods (30 days before anthesis, 30 days after anthesis, and ±30 days around anthesis) as well as throughout the entire season. Nitrogen fertilizer treatments ranged from zero to 140 kg N ha^{-1}. The model accurately simulated yields with an RMSE of 895.5 kg ha^{-1} during calibration and 1091.4 kg ha^{-1} during validation. Results showed that yields were not adversely affected by rainfall reductions up to 40 %, regardless of N levels or timing. However, yields significantly declined when reductions exceeded 60 %, especially with N applications above 100 kg ha^{-1}. Optimal yields were noted at 140 kg N ha^{-1}, but benefits decreased under scenarios of reduced rainfall, indicating that N recommendations may need to be lowered in response to projected rainfall reductions. This study provides quantitative guidance for adapting wheat fertilization strategies to maintain productivity while accounting for future rainfall variability.

1. Introduction

Wheat (*Triticum aestivum* L.) is a staple crop worldwide, covering 219 million hectares with an average yield of almost 3.7 t ha^{-1} (at 11 % moisture content), resulting in a global production of 808 million tons (Peña-Bautista et al., 2017). Switzerland contributes 487 thousand tons to this total, with an average yield of 5.4 t ha^{-1} (FAOSTAT, 2022). However, wheat-growing regions in Switzerland are projected to face more intense rainfall during winter and spring, along with hotter and drier summers, potentially reducing rainfall by up to 43 % by the end of the century (CH2018, 2018; Fischer et al., 2022). While increased atmospheric carbon dioxide (CO_2) levels associated with climate change could theoretically enhance photosynthesis and promote wheat growth, this carbon fertilization effect is diminished under water-limited conditions (Zheng et al., 2020). Drought exerts a significant negative impact on wheat yield (Fuhrer et al., 2006), particularly in Europe (Webber et al., 2018). It impacts wheat plants in various ways, including reduced CO_2 uptake and impaired photosynthetic performance due to stomatal limitations (Zandalinas et al., 2018). During early reproductive phases, drought can severely hinder grain production (Onyemaobi et al., 2017) and significantly affect overall yield (Ji et al., 2010; Qaseem et al., 2019), while drought during grain filling can compromise grain development (Steduto et al., 2012). However, the current understanding of the rainfall sensitivity of wheat at different reproductive stages remains inconsistent, highlighting a gap in knowledge.

Addressing this gap also requires considering how nitrogen (N) interacts with water availability, since globally, wheat production faces a major challenge: only about 48 % of the N fertilizer applied is recovered by plants (Ladha et al., 2016), with efficiency varying widely between regions and even between farms within the same area (Ladha et al.,

* Corresponding author at: Agroscope, Plant Production Systems, Route de Duillier 60, Nyon 1260, Switzerland.
E-mail address: paola.bongiovani@agroscope.admin.ch (P.F. Bongiovani).

https://doi.org/10.1016/j.eja.2025.127728
Received 25 February 2025; Received in revised form 1 June 2025; Accepted 1 June 2025
Available online 13 June 2025

2005). This inefficiency not only limits yield and grain protein potential (Steduto et al., 2012; Zörb et al., 2018), but also contributes to serious environmental problems, including groundwater and waterways contamination, and greenhouse gas emissions (Zörb et al., 2018). To mitigate these issues, N application must be reduced in accordance with the European Union's Nitrates Directive (91/676/EEC), which was established in 1991 to prevent water pollution from agricultural sources (EU Commission, 1991). Despite these environmental concerns, limited N availability during wheat growth can compromise both yield and grain quality. For instance, a global meta-analysis revealed that applying N at rates up to 200 kg N ha^{-1} can substantially enhance wheat yields (by 37.6 % at 0–100 kg N ha^{-1} and by 49.5 % at 100–200 kg N ha^{-1}) with significant improvements in grain protein content (Wang et al., 2023). Furthermore, according to Martre et al. (2024), the attainment of global wheat yield potential under a mid-century high-warming climate change scenario with elevated CO_2 needs an increase in N fertilizer application to four times the current levels. Yet, adding more N does not always translate into greater yields. Excessive applications can lead to vegetative overgrowth and increase water use (Steduto et al., 2012), due to elevated canopy-level transpiration, leading to the risk of water stress (Nguyen et al., 2022). In regions where water availability constrains crop productivity, elevated N rates may exacerbate water stress without improving yields. Adjusting future N rates to anticipated rainfall, especially considering expected reductions due to climate change, is recommended. Nevertheless, current N fertilizer recommendations are mostly based on inter-annual average responses, often ignoring the variations induced by stage-specific drought events (Asseng et al., 2012), thus limiting their effectiveness under climate change scenarios. A better understanding of the phased drought × N interaction is therefore critical to improve wheat yield resilience.

Process-based crop simulation models (CMs) are often used as valuable tools for studying climate change impacts on agriculture. CMs are composed of mathematical equations that estimate the growth, development, and yield of crops based on environmental factors such as climate and soil, genetic traits of cultivars, and management practices (Monteith, 1996). These models are capable of simulating crop growth under both current and future scenarios (Finger and Schmid, 2008), and can be calibrated and validated using data from field experiments, which is crucial for improving model accuracy (Hunt and Boote, 1998). Additionally, CMs can be applied to study various locations and climatic conditions (Jones et al., 2003). In the context of climate change, CMs are essential tools for predicting how crops will respond to shifting environmental conditions (Lehmann et al., 2013) and for evaluating strategies to mitigate adverse impacts on yields (Matthews et al., 2013). However, accurately replicating future climate conditions in field experiments remains challenging (Bongiovani et al., 2024), further reinforcing the importance of simulation approaches. Using CMs, Pequeno et al. (2021) demonstrated how region-specific adaptation strategies and soil N management can enhance the performance of heat and drought tolerant wheat varieties under climate change. Despite their advantages, CMs present inherent uncertainties related to system complexity, parameter adjustment needs, and input data variability (Battisti, 2016; Duarte, 2018; Duarte and Sentelhas, 2020). Among the leading systems employing CMs is the Decision Support System for Agrotechnology Transfer (DSSAT), version 4.8.2.000 (Hoogenboom et al., 2024; Hoogenboom et al., 2019; Jones et al., 2003). The DSSAT-Nwheat model (Kassie et al., 2016), is based on the Crop Environment Resource Synthesis model, or CERES (Ritchie et al., 1998), and has been widely used for simulating wheat growth and yield under different environmental conditions (Holzworth et al., 2014; Asseng et al., 1998; Kassie et al., 2016; Liu et al., 2020; Shoukat et al., 2024). Its strength lies in its ability to simulate wheat responses under different N and water conditions, making it particularly suitable for assessing wheat resilience to climate change scenarios (Asseng et al., 2013; Jägermeyr et al., 2021; Pequeno et al., 2021; Martre et al., 2024). Successful application of these models, however, depends on effective calibration using detailed field experiments (Nóia Júnior et al., 2023a; Kim et al., 2024), which ensures that simulations better reflect reality. Therefore, well-calibrated and validated CMs are critical tools for assessing future crop yields under changing climate conditions, particularly in scenarios of reduced rainfall.

The present study specifically addresses these gaps by calibrating and evaluating the DSSAT-Nwheat model for the Swiss wheat genotype CH Nara, aiming to quantify the impacts of reduced rainfall and N fertilizer inputs on wheat yields under a warm-summer humid continental climate. The following two hypotheses will be tested: (1) the effects of reduced rainfall and lower N fertilizer inputs on wheat yield vary depending on the timing of rainfall reduction; and (2) higher N fertilizer rates (≥100 kg N ha^{-1}) increase wheat yield sensitivity to rainfall reduction, particularly during critical growth stages. These analyses aim to provide insights into how climate variability and resource management interact to influence wheat yield under current and projected climatic conditions, thus supporting more resilient wheat production systems in Switzerland and similar environments.

2. Material and methods

2.1. Weather and soil data

The Köppen's climate classification for the region is warm-summer humid continental climate (Cfb, Beck et al., 2018). Meteorological data was obtained from the local weather station of MeteoSwiss for the historical period of 1981–2022 (Historical Series; hereinafter referred to as "HS"). Considering the 42-year-period, the mean annual temperature was 9.2 °C, the mean annual rainfall was 831.6 mm, and the mean annual solar radiation, 11.8 MJ m^{-2} d^{-1}. Mean historical weather conditions during the winter wheat growing season, as well as the conditions during the years of field experiment are shown in Fig. 1.

The soils of the field experiments were classified as Cambisols (WRBSR World Reference Base for Soil Resources, 2014). Soils were sampled with an auger on November 08 and 9, 2023, considering three samples that were mixed and created one unique sample for each plot per each depth: 0–20 cm, 20–40 cm, 40–60 cm and, when possible, 60–80 cm. In certain plots, the presence of subsurface rock layers inhibited sampling depths beyond 60 cm. Soil samples were sent to an external lab (Sol-Conseil, Gland, Switzerland) and analyzed for: texture, organic matter, and pH measured in water (pH_{water}, Table 1).

2.2. Field experiments

Two field experiments, EXP1 (Bongiovani et al., 2024) and EXP2 (Burton et al., 2024), were carried out between September 2018 and July 2022, in Nyon, Switzerland (46.39 °N, 6.24 °E, 424 m a.s.l). In EXP1, winter wheat was cultivated in three nearby plots after three pre-crops (barley, *Hordeum vulgare* L.; oilseed rape, *Brassica napus* L.; winter pea, *Pisum sativum* L.), while in EXP2, only one crop preceded winter wheat each season, either sunflower (*Helianthus annuus*) or soybean (*Glycine max*) (Table 2). The drought tolerant (Touzy et al., 2019) Swiss winter wheat genotype CH Nara, registered in 2007, was cultivated in both experiments. It is among the top Swiss varieties of winter wheat, which generally present high protein content and baking qualities (Brabant and Levy Häner, 2016). CH Nara is also resistant to lodging and diseases, like brown and yellow rust, and considered very short compared to other genotypes cultivated in Switzerland (ARVALIS, 2025). The experimental observed data used in this study included: anthesis and maturity dates, grain yield, grain number per m^2, individual grain weight, grain N content (from EXP1 and EXP2), and total aboveground biomass at maturity (only available in EXP2) (Supp. Tab. S1 and S2).

Among the main objectives of these experiments was the investigation of wheat yields in response to different mineral N management levels, under no limitation of phosphorus and potassium. The N

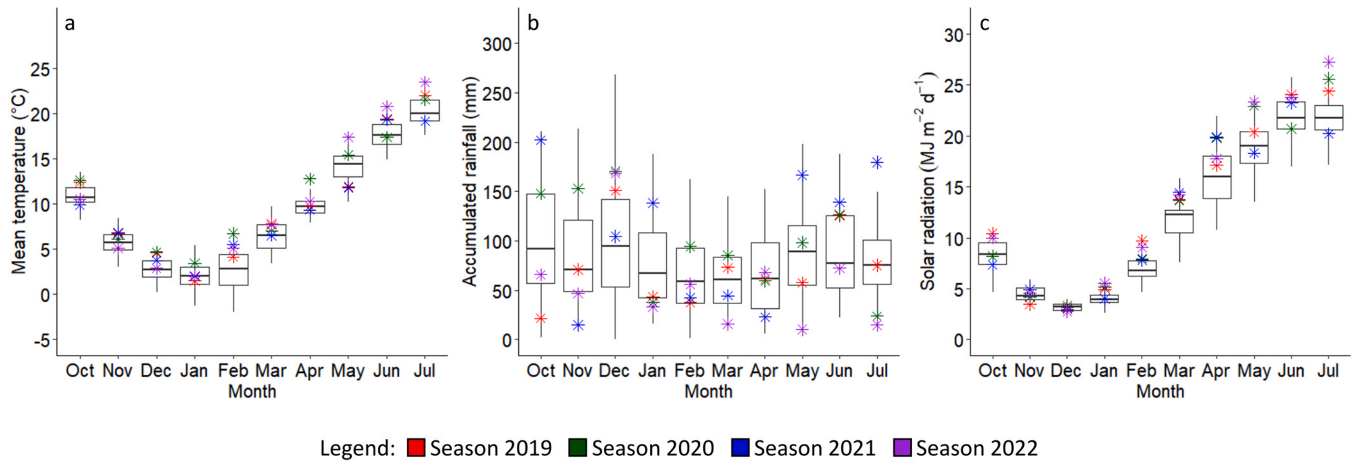

Fig. 1. Weather conditions during winter wheat cropping seasons in Nyon, Switzerland. Boxplot of monthly mean temperature (a), accumulated rainfall (b) and solar radiation (c), over the HS period in Nyon, Switzerland, and standard error of the means. Weather data corresponding to the growing seasons of the wheat field experiments (from October to July) are shown as red, green, blue and purple asterisks for seasons 2019, 2020, 2021 and 2022 (years of harvest), respectively. Data from MeteoSwiss, the Swiss Federal Office for Meteorology and Climatology.

Table 1
Selected soil properties of the plots where the experiments were carried out. Soil depth, concentration of clay, silt, sand, organic matter (OM), and pH_{water}, of EXP1 and EXP2.

Soil code	Depth (cm)	Clay	Silt	Sand	OM (g 100 g^{-1})	pH_{water}	Experiment
		(g 100 g^{-1})					
Soil1	0–20	29.0	44.1	26.9	2.8	6.4	EXP1
	20–40	30.2	44.3	25.5	1.9	6.6	
	40–60	41.9	35.5	22.6	1.5	6.8	
	60–80	37.9	42.6	19.5	1.0	7.0	
Soil2	0–20	33.0	35.6	31.5	3.1	7.8	EXP2
	20–40	31.4	34.9	33.7	2.9	7.8	
	40–60	32.3	36.9	30.7	2.1	8.0	
Soil3	0–20	26.9	40.6	32.5	3.0	8.0	
	20–40	26.5	43.3	30.2	2.2	8.1	
	40–60	27.1	42.3	30.6	1.7	8.1	
	60–80	26.0	43.1	30.9	1.4	8.3	
Soil4	0–20	28.9	42.4	28.7	2.9	7.5	
	20–40	30.9	38.4	30.7	2.4	7.5	
	40–60	32.4	27.9	39.7	1.8	7.9	
Soil5	0–20	58.7	30.5	10.8	4.4	7.3	
	20–40	47.1	34.9	18.1	2.6	7.5	
	40–60	46.5	31.4	22.0	1.6	7.7	

Table 2
Field management for the winter wheat genotype CH Nara experiments in Nyon, Switzerland, and use in calibration of the DSSAT-Nwheat model. Sowing, anthesis, maturity, harvest, nitrogen (N) fertilization dates and N fertilizer input in wheat production by experiment (EXP1 and EXP2) and season (season 2019, 2020, 2021 and 2022). More information about the treatments and in each phase of the calibration of the model they were used can be found in Supplementary Tab. S1, S2 and S3.

Operation	EXP1	EXP2			
	2019	2019	2020	2021	2022
Soil	Soil1	Soil2	Soil3	Soil4	Soil5
Pre-crop	barley oilseed rape peas	sunflower	soybean	soybean	sunflower
Sowing	19 Oct 2018	11 Oct 2018	13 Nov 2019	06 Nov 2020	15 Oct 2021
N fertilizer input (kg N ha^{-1})	0 up to 180	0 160	0 160	0 80 160	0 80 160
N supply date	27 Mar 2019 06 May 2019	21 Feb 2019 21 Mar 2019 02 May 2019	18 Feb 2020 17 Mar 2020 04 May 2020	24 Feb 2021 23 Mar 2021 20 Apr 2021	28 Feb 2022 25 Mar 2022 03 May 2022
Water supply	Rainfed Shelter	Irrigation	Rainfed	Rainfed	Irrigation
Harvest	22 Jul 2019	17 Jul 2019	15 Jul 2020	23 Jul 2021	07 Jul 2022
Phases	Calibration Evaluation	Calibration Evaluation	Calibration Evaluation	Calibration Evaluation	Evaluation

treatments ranged from non-fertilized (zero N fertilizer supply) to 160 kg N ha^{-1}, and to enough mineral N applied to reach a total soil supply of 180 kg N ha^{-1}. Soil samples were collected on February of 2019, 2020, 2021, and 2022, at beginning of tillering of both experiments, as well as at after harvest in EXP2, to quantify the soil mineral N (NO_3^- plus NH_4^+, hereafter referred to as Nmin) by an external lab. Then, the Nmin system by Thompson et al. (2017) was applied in EXP1, in which the determined Nmin at the beginning of wheat development was subtracted from the N target value (180 kg N ha^{-1}) to estimate the mineral N fertilizer application rate (Bongiovani et al., 2024). Ammonium nitrate (27 % N + 2.5 % Mg) was broadcast twice in EXP1 by the time of stem elongation and heading stages (due to an initial Nmin of 50 kg N ha^{-1} after peas, and 110 kg N ha^{-1} after barley and oilseed rape), and three times in EXP2, by the time of tillering, stem elongation and heading stages.

Another objective of EXP1 was to test the effects of the future projections of rainfall reductions. Thus, EXP1 presented the treatments: rainfed and rainfall manipulation with rainout shelters (Table 2). The stationary rainout shelters were built and installed to specifically intercept up to 40 % of the rainfall, based on the design used by Kundel et al. (2018). The rainout shelters covered plots continuously during the grain filling stage, a critical stage for wheat yield, being uncovered during all other growth stages. Although EXP2 was a rainfed experiment, due to severe drought, irrigation was applied in season 2019 (20 mm on 18 October 2018) to ensure plant emergence, and in 2022 (25 mm on 25 May 2022), to minimize a potential water stress at the final winter wheat stages after a lower-than-average rainfall accumulation during summer (Fig. 1). Detailed information about the methods used and the field assessments conducted for EXP1 and EXP2 is available in Bongiovani et al. (2024) and Burton et al. (2024), respectively.

2.3. Calibration and evaluation of the DSSAT-Nwheat model for CH Nara genotype

The DSSAT-Nwheat model is integrated within the Decision Support System of Agrotechnology Transfer modelling system, or DSSAT (version 4.8.2.000, Hoogenboom et al., 2024; Jones et al., 2003), a crop model developed for the simulation of winter wheat growth (Kassie et al., 2016). DSSAT-Nwheat was selected for its proven ability to simulate wheat growth, development, and yield under diverse N levels, water regimes, planting dates, elevated CO_2, temperature variations, and soil types worldwide (Kassie et al., 2016). The model has been comprehensively validated with over 1000 observations from 65 treatments, achieving a root mean square deviation (RMSD) of 0.89 t ha^{-1} (13 %) for grain yield. It reliably captures the impacts of N and water management, as well as responses to temperature and CO_2 changes, making it well-suited for climate-N impact studies. Furthermore, DSSAT-Nwheat simulates wheat phenology and resource use efficiency in detail, allowing the analysis of water and N stress at specific growth stages, which is essential for investigating phased drought × N interactions.

For the calibration of the model, results of experiments, seasons and treatments with no or minimum water and N stress were considered. So, in this phase, the fertilized treatments of 2019 from EXP1, and N treatments of 80 kg N ha^{-1} and 160 kg N ha^{-1} of seasons 2019, 2020 and 2021 from EXP2, were used (Table 2, Supp. Tab. S1 and S2). For the evaluation of the calibration, the season 2021 from EXP1, the season 2022 from EXP2, the non-fertilized treatments (zero N fertilizer supply) of both EXP1 and EXP2, as well as the remaining 80 kg N ha^{-1} treatments (EXP2), were used (Table 2, Supp. Tab. S1 and S2).

The rainout shelters' treatments were set up to intercept 40 % of the rain during the period the shelters were in the field (Bongiovani et al., 2024). Initial water availability of 75 % and soil N conditions were established 15 days before sowing in DSSAT, to achieve the Nmin found in field experiments each season. Based on the soil properties shown in Table 1, other soil parameters needed for running the model were calculated automatically by the DSSAT's soil module, creating the soil profiles. The soil parameters include: water content at lower limit (LL, cm^3 cm^{-3}), water content at drained upper limit (DUL, cm^3 cm^{-3}), saturated water content (SAT, cm^3 cm^{-3}), root growth factor (RGF, %), saturated hydraulic conductivity (SKS, cm hr^{-1}), soil density (BDM, g cm^{-3}), organic carbon (LOC, %), clay (LCL, %), silt (LSI, %), coarse fraction (LCF, %), N concentration (LNI, %), pH in water (LHW), and cation exchange capacity (CEC, cmol kg^{-1}). The soil profiles created were used for all the simulations and can be found in Supplementary Tab. S4 to S8.

The DSSAT-Nwheat model presents nine cultivar coefficients to be adjusted during calibration phase. The coefficients descriptions, as shown in the DSSAT platform, are: VSEN is the sensitivity to vernalization; PPSEN is the sensitivity to photoperiod; P1 is the thermal time from seedling emergence to the end of the juvenile phase (°C d); P5 is the thermal time (base 0 °C) from beginning of grain filling to maturity; PHINT is the phyllochron interval; GRNO is the number of kernels per stem weight at grain filling (kernels g^{-1} stem^{-1}); MXFIL is the potential kernel growth rate (mg kernel^{-1} d^{-1}); STMMX is the potential final dry weight of a single tiller without grain (g); and SLAP1 is the ratio of leaf area to mass at emergence (cm^2 g^{-1}). The genotype parameters for CH Nara were initially simulated with the GLUE (generalized likelihood uncertainty estimation) tool available in DSSAT, using the available observed data. Calibration error control criteria were defined as minimizing the root mean square error (RMSE) and maximizing the coefficient of determination (R^2) between observed and simulated grain yield, anthesis date, and maturity date. All calibrated parameters were kept within the default minimum and maximum ranges suggested by DSSAT-Nwheat (Table 3). Then, they were adapted to improve the relationship between observed and simulated data. The cultivar coefficients of the winter wheat genotype CH Nara for the DSSAT-Nwheat model are shown in Table 3.

2.4. Simulations

The simulations were performed for the location of the field experiments. Forty-two years of winter wheat production were simulated using all five soils (Table 1), to represent the variability of the region, as well as the HS weather data (1981–2022). The simulations were carried out for the calibrated genotype CH Nara. Sowing was set as October 15 each year, while harvest occurred automatically at plant maturity on the following year, a date that varied according to the seasons' conditions. In order to simulate the region's water availability conditions during wheat production, the simulation start date was set as 180 days before sowing.

Besides the actual HS rainfall treatment, five other rainfall treatments were created to simulate reduced rainfall conditions, being −20 % (R20), −40 % (R40), −60 % (R60), −80 % (R80) and −100 % (R100) of the HS's rainfall. Each reduced rainfall condition was applied on three different phases around anthesis (scenarios): stem elongation (30 days before and including the anthesis date, totalizing 31 days), end of flowering and grain filling (30 days after and including the anthesis date, totalizing 31 days), and between stem elongation and grain filling (30 days before and after anthesis, including it, totalizing 61 days). The 30 days period was decided based on the number of days found from anthesis to maturity of the field experiments (32–45 days, Supp. Tab. S1 and S2), so each simulated year would have the same number of days of rainfall reductions. Additionally, a fourth scenario was created to simulate decreases of rainfall during the entire growing season, from the sowing date to maturity (or end of July). The average anthesis date observed on the field experiments was 220 ± 9.7 days after sowing (DAS) (Supp. Tab. S1 and S2), thus set as May 22 (disregarding leap years). Projections of other weather variables were not considered in this study.

Four N treatments were considered in each rainfall treatment: zero N supply (N0), 60 kg N ha^{-1} (N60), 100 kg N ha^{-1} (N100) and 140 kg N

Table 3
Default (minimum and maximum) and calibrated cultivar coefficients values of winter wheat genotype CH Nara for DSSAT-Nwheat (v. 4.8.2.000).

Genotype	Cultivar coefficients								
	VSEN	PPSEN	P1	P5	PHINT	GRNO	MXFIL	STMMX	SLAP1
$Default_{min}$	0	1.20	380.0	200.0	85.0	20.0	1.60	1.00	200.0
$Default_{max}$	4.00	4.50	530.0	700.0	130.0	32.0	2.90	3.00	400.0
CH Nara	1.00	4.0	500.5	550.0	86.3	25.0	1.80	3.00	250.0

ha^{-1} (N140), the latter represents the recommended N fertilizer input for winter wheat production in Switzerland (PRIF, Sinaj et al., 2017). The N doses were split in three applications based on the application dates of the field experiments (Table 2) and the plants needs in each development phase: February 23, March 22 and May 4. On N60, the doses applied were 20 kg N ha^{-1} in each application. On N100, the doses were 30 kg N ha^{-1}, 40 kg N ha^{-1} and 30 kg N ha^{-1}. For the N140, the doses were 40 kg N ha^{-1}, 60 kg N ha^{-1} and 40 kg N ha^{-1}. Ammonium nitrate was broadcast in each N application and no other fertilizer was added to the simulations.

For the analysis of simulation outcomes, the following variables were considered: yield, grain number per m^2, individual grain weight (mg), total aboveground biomass (kg ha^{-1}), N in grain (kg ha^{-1}), N in straw (kg ha^{-1}), leaf area index (LAI), and grain protein content (g 100 g^{-1} dry matter), which was calculated from the N content output of the model using a conversion factor of 5.7 (Schulz et al., 2015). These variables are critical as they directly reflect crop productivity and quality. Based on them, the N harvest index (NHI, defined as the proportion of N allocated to grain relative to the total N in grain and straw) and N utilization efficiency (NUtE, defined as the grain yield per unit of total N in grain and straw) were calculated. To further investigate the N dynamics in the simulations, additional output variables generated by the model were analyzed: plant N uptake (kg N ha^{-1}) and N leached (kg N ha^{-1}). These variables represent key processes computed in the soil inorganic N module of DSSAT on a daily basis. The model calculates plant uptake rates for NO_3^- and NH_4^+ in the individual plant modules, integrating the amounts taken up into the soil state variables of the inorganic N module. The transport of N in soil to deeper layers is based on water flux values obtained from the soil water module (Jones et al., 2003; Hoogenboom et al., 2024).

3. Statistical analysis

The performance of the model in relation to the observed data was verified based on the statistical indicators: agreement index (d) of Willmott (1982), coefficient of determination (R^2), root mean square error (RMSE) and relative root mean square error (RRMSE). These indices are obtained by Eqs. 1 to 4.

$$d = 1 - \left[\frac{\sum (E_i - O_i)^2}{\sum(|E_i - \overline{O}| + |O_i - \overline{O}|)^2}\right] \tag{1}$$

$$R^2 = 1 - \frac{\sum(E_i - \overline{O})^2}{\sum(O_i - \overline{O})^2} \tag{2}$$

$$RMSE = \sqrt{\frac{\sum(E_i - O_i)^2}{n}} \tag{3}$$

$$RRMSE = \frac{RMSE}{\overline{O}} \times 100 \tag{4}$$

Where: E_i corresponds to the values simulated by the models; O_i, to the observed values; $\bar{O}$ is the average of the observed values; and n is the total number of observed or simulated values.

Boxplots were created to show the winter wheat grain number, weight and yield simulations by scenario of rainfall reduction. To evaluate the effects of rainfall reduction, N supply, and their interaction on grain number, grain weight, and grain yield, a two-way analysis of variance (ANOVA) was performed using linear models, applying the type II sum of squares to evaluate the main and interaction effects, which accounts for variance explained by each factor while controlling for the other. ANOVA was conducted using the function "Anova" from the "car" package in R (version 4.4.2, R core Team, 2024), applied to linear models fitted with "lm" function. Statistical significance was evaluated at $\alpha = 0.05$. The ANOVA tables are available in Supplementary Materials.

Additionally, a Principal Component analysis (PCA), to assess differences between main factors and their interactions, was carried out in R (version 4.4.2, R Core Team, (2024). It was used to reduce the dimensions of the dataset and better visualize correlations between variables using the function "prcomp" in R. The variables used in this analysis were: wheat grain yield (kg ha^{-1}), grain number (grains per m^2), individual grain weight (mg), total aboveground biomass (kg ha^{-1}), N in grain (kg ha^{-1}), N in straw (kg ha^{-1}), leaf area index (LAI), grain protein content (g 100 g^{-1} dry matter), NHI, NUtE, plant N uptake (kg N ha^{-1}), and soil N leached (kg N ha^{-1}). The PCA included all the sources of variation at a similar level. The results were plotted using the function "autoplot", from the R package "ggfortify". Nitrogen fertilizer supply, rainfall reduction and scenario of rainfall reductions were highlighted in plots to assess differences between them. Only the first two principal components were illustrated in these plots since they accounted for most of the variation in the data in all cases. To quantitatively assess the significance of sample separation according to each experimental factor, a separate Permutational Multivariate Analysis of Variance (PERMANOVA) was performed on the PCA scores (PC1 and PC2) for N supply, rainfall reduction, and scenario of rainfall reductions, respectively. PERMANOVA was conducted using the function "adonis2" from the R package "vegan". The Euclidean distance matrix was used for each analysis, and significance was assessed based on 999 permutations. In PERMANOVA, the R^2 value represents the proportion of variation in a distance matrix explained by grouping factors. Unlike the R^2 defined in Eq. 2, it operates on pairwise distances without assuming linearity or normality. It quantifies explanatory power in a multivariate, non-parametric framework, with significance tested by permutations.

4. Results

4.1. Calibration and evaluation of DSSAT-Nwheat

In the calibration phase, the model could simulate different crop variables appropriately (Table 4, Supp. Fig. S1). Phenological stages, represented by anthesis and maturity dates, were simulated with high accuracy (d > 0.951) and precision (R^2 > 0.838), with RRMSE ranging from 1.2 % to 2.1 %. Yield simulates had an agreement index of d = 0.759, with an R^2 of 0.517 and an RMSE of 895.5 kg ha^{-1}. The mean observed yield from field experiments was 5570.5 kg ha^{-1}, while the model simulated an average yield of 6139.6 kg ha^{-1}. Total aboveground biomass showed lower agreement, with d = 0.252 and R^2 = 0.295. For other variables, accuracy ranged from d = 0.478–0.619, while precision, represented by R^2, ranged from 0.143 for grain number to 0.393 for grain weight.

In the evaluation phase, both anthesis (d = 0.982 and R^2 = 0.979) and maturity dates (d = 0.961 and R^2 = 0.867) were accurately and precisely simulated by the model, while other variables were often underestimated (Table 4, Supp. Fig. S1). The precision of vegetative

Table 4
Statistical analysis of observed and simulated values of CH Nara. Observed (Obs.) and simulated (Sim.) anthesis and maturity date (in days after sowing), total aboveground biomass (in t ha^{-1}), grain (G.) number per m^2, grain weight (in mg) and grain nitrogen (N) content (in g per 100 g of dry matter or DM), and yield (in t ha^{-1}) for the DSSAT-Nwheat model calibrated for the winter wheat genotype CH Nara.

Variable	Unit	Obs. Mean ±standard error	Sim. Mean ±standard error	d	R^2	RMSE (Unit)	RRMSE (%)
			Calibration				
Anthesis	DAS	216.8 ± 3.2	218.3 ± 3.5	0.991	0.981	2.5	1.2
Maturity	DAS	256.4 ± 3.5	256.4 ± 3.0	0.951	0.838	5.5	2.1
Biomass	t ha^{-1}	19.5 ± 0.3	17.6 ± 0.2	0.295	0.252	2753.3	14.1
G. number	G. m^{-2}	14699.0 ± 360.6	15797.9 ± 448.7	0.616	0.143	2084.7	14.2
G. weight	mg	37.8 ± 1.2	38.9 ± 0.5	0.619	0.393	3.8	10.1
G. N content	g 100 g^{-1} DM	2.37 ± 0.07	1.94 ± 0.04	0.478	0.152	0.5	21.2
Yield	t ha^{-1}	5.5 ± 0.2	6.1 ± 0.1	0.759	0.517	895.5	16.1
			Evaluation				
Anthesis	DAS	220.5 ± 1.6	222.2 ± 1.8	0.982	0.979	2.3	1.0
Maturity	DAS	259.8 ± 1.8	259.6 ± 1.6	0.961	0.867	3.2	1.2
Biomass	t ha^{-1}	12.7 ± 0.5	10.3 ± 0.6	0.596	0.156	3907.9	30.6
G. number	G. m^{-2}	11727.1 ± 542.2	9479.9 ± 424.1	0.704	0.548	2876.0	24.5
G. weight	mg	38.8 ± 0.8	37.4 ± 0.7	0.232	0.061	5.9	15.1
G. N content	g 100 g^{-1} DM	2.05 ± 0.06	1.75 ± 0.03	0.348	0.154	0.5	24.0
Yield	t ha^{-1}	4.5 ± 0.2	3.5 ± 0.2	0.742	0.660	1091.4	24.3

variables varied, with R^2 values ranging from 0.061 for grain weight to 0.660 for yield, and RRMSE between 15.1 % for grain weight and 30.6 % for total aboveground biomass (Table 4). Accuracy was highest for yield (d = 0.742), followed by grain number (d = 0.704), total aboveground biomass (d = 0.596), grain N content (d = 0.348), and grain weight (d = 0.232). Additionally, in both calibration and simulation phases, the model produced similar simulated values for a wide range of observed values in the field. For instance, during calibration, observed grain weight values ranged from 29.8 mg to 34.3 mg, whereas the corresponding simulated values were between 37.0 mg and 37.2 mg (Supp. Tab. S1 and S2, Supp. Fig. S1).

4.2. Winter wheat grain number, weight and yield simulations

4.2.1. Rainfall decreases during stem elongation

The simulated responses of winter wheat to reduced rainfall 30 days before anthesis with different N fertilizer supply is shown in Fig. 2. In this scenario, considering all N treatments together, means of both grain number and yield decreased with rainfall reductions, while grain weight means, had variable responses. The greatest mean grain number was obtained in HS (10,435.6 grains m^{-2}), followed by R20 (10,416.1 grains m^{-2}), R40 (10,329.0 grains m^{-2}), R60 (10,094.7 grains m^{-2}), R80 (9616.0 grains m^{-2}), and R100 (8742.5 grains m^{-2}). As for the yields, the greatest mean was observed in HS (4.06 t ha^{-1}), followed by R20 (4.04 t ha^{-1}), R40 (3.97 t ha^{-1}), R60 (3.85 t ha^{-1}), R80 (3.67 t ha^{-1}), and R100 (3.48 t ha^{-1}). Grain weight means varied between rainfall reduction levels, being greater in R100 (38.1 mg), followed by HS (37.1 mg), R20 (37.0 mg), R40 (36.8 mg), R80 (36.6 mg), and R60 (36.5 mg). The N0 treatment presents more consistent results along the different rainfall levels than the other N treatments, for the three variables.

When comparing the N treatments (Supp. Tab. S9), the N140 had the greatest means of grain number and yield in all rainfall reduction levels, while N0 had the lowest. In N140, grain numbers went from 10,530.4 grains m^{-2} (R100) to 13,353.5 grains m^{-2} (HS), and yields from 4.22 t ha^{-1} (R100) to 5.29 t ha^{-1} (HS). In N0, grain numbers went from 5790.6 grains m^{-2} (R100) to 6144.0 grains m^{-2} (R40), and yields from 2.11 t ha^{-1} (R100) to 2.28 t ha^{-1} (R40). N60 and N100 had intermediary responses, with N100 being greater than N60 in all cases. The N60 had its greatest values in R20 (10,283.6 grains m^{-2} and 3.93 t ha^{-1}), and lowest in R100 (8699.6 grains m^{-2} and 3.55 t ha^{-1}), while N100 had its greatest values in HS (12,081.8 grains m^{-2} and 4.81 t ha^{-1}), and lowest in R100 (9949.2 grains m^{-2} and 4.03 t ha^{-1}). As for the grain weight, its greatest means were obtained by N100, in all levels except in R100, while the lowest, by N0. N140 had grain weights from 36.9 mg (R60) to 38.8 mg (R100), N100 from 37.3 mg (R80) to 39.2 mg (R100), N60 from 36.4 mg (R60) to 39.5 mg (R100), and N0, from 35.1 mg (R100) to 35.4 mg (both R40 and R60).

Analysis of variance confirmed that rainfall reduction, N supply, and their interaction significantly affected grain number and grain yield ($p < 0.001$ for all effects). For grain weight, N supply and rainfall reduction were significant factors ($p < 0.001$ and $p = 0.014$, respectively), but their interaction was not significant ($p = 0.744$, Supp. Tab. S9).

4.2.2. Rainfall decreases during end of flowering and grain filling

The simulated responses of winter wheat to reduced rainfall 30 days after anthesis with different N fertilizer supply is shown in Fig. 3. In this scenario, considering all N treatments together, means of both grain weight and yield decreased with rainfall reductions, while grain number means were greater in R20 and R40 than in HS. As in the previous scenario, the greatest yield mean occurred in HS (4.06 t ha^{-1}). It was followed by the rainfall reductions levels of R20 (4.00 t ha^{-1}), R40 (3.90 t ha^{-1}), R60 (3.74 t ha^{-1}), R80 (3.51 t ha^{-1}), and R100 (3.30 t ha^{-1}). The grain weight means had similar tendence, being greater in HS (37.1 mg), followed by R20 (36.5 mg), R40 (35.5 mg), R60 (34.2 mg), R80 (32.4 mg), and R100 (31.1 mg). As for the grain numbers, as mentioned, was greater in R20 (10,451.6 grains m^{-2}) and R40 (10,447.1 grains m^{-2}), than in HS conditions (10,435.6 grains m^{-2}). Then, it decreased with rainfall reductions, with 10,409.6 grains m^{-2} in R60, 10,308.0 grains m^{-2} in R80, and 10,166.2 grains m^{-2} in R100. The N0 treatment presents more consistent results along the different rainfall levels than the other N treatments, especially for grain number and yield.

Considering the N treatments (Supp. Tab. S10), the N140 had the greatest means of grain number and yield in all rainfall reduction levels, while N0 had the lowest. In N140, grain numbers went from 12,673.3 grains m^{-2} (R100) to 13,353.5 grains m^{-2} (HS), and yields from 3.95 t ha^{-1} (R100) to 5.29 t ha^{-1} (HS). In N0, grain numbers went from 6035.1 grains m^{-2} (HS) to 6169.3 grains m^{-2} (R80), and yields from 2.02 t ha^{-1} (R100) to 2.23 t ha^{-1}, in both HS and R20. N60 and N100 had intermediary responses, with N100 being greater than N60 in all cases. N60 mean yields went from 3.84 t ha^{-1} (R100) to 4.81 t ha^{-1} (HS), and mean grain numbers, from 10,152.2 grains m^{-2} (R100) to 10,310.3 grains m^{-2} (R40). N100 mean yield went from 3.37 t ha^{-1} (R100) to 3.92 t ha^{-1} (HS), and mean grain number, from 11,725.3 grains m^{-2} (R100) to 12,081.8 grains m^{-2} (HS). As for the grain weight, the lowest mean of every N treatment occurred in R100, while the greatest, in HS. N140 had

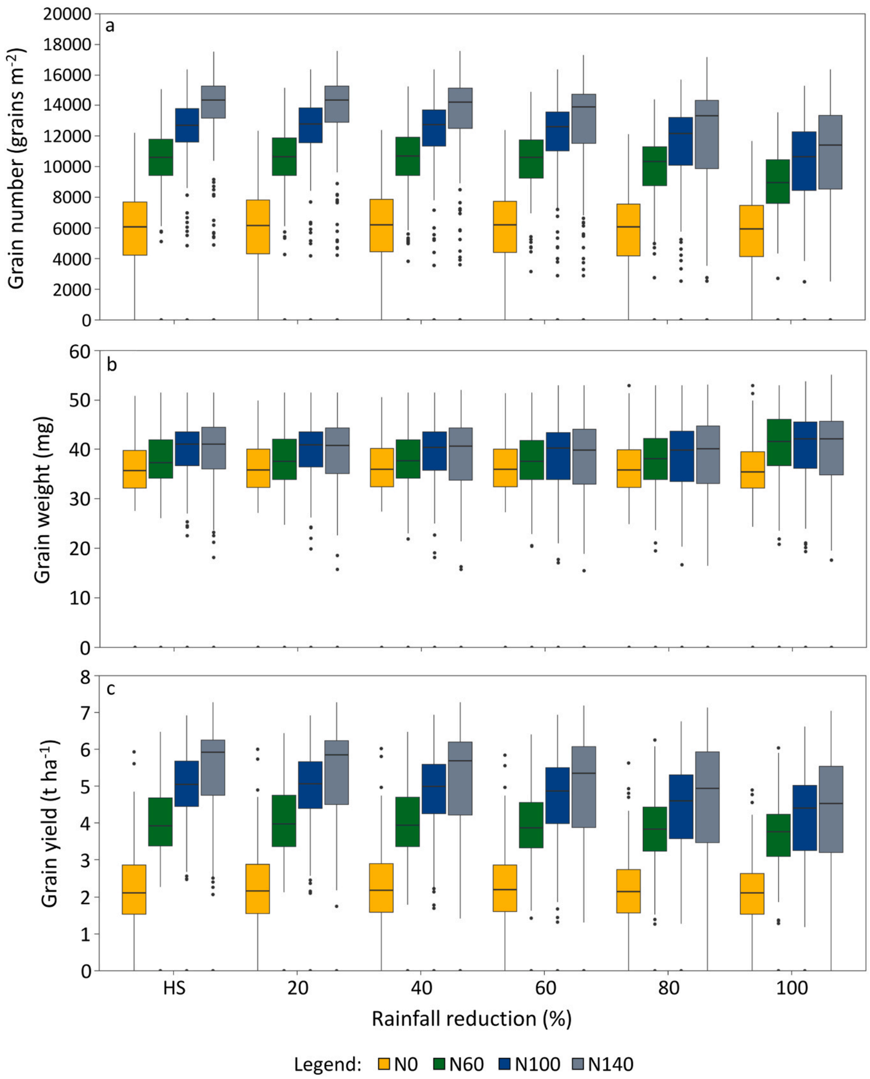

Fig. 2. Simulated responses of winter wheat to reduced rainfall 30 days before anthesis under four nitrogen fertilizer supplies. Winter wheat grain number (a), grain weight (b) and yield (c) responses to reductions of rainfall of 20 % (R20), 40 % (R40), 60 % (R60), 80 % (R80) and 100 % (R100) of the Historical Series (HS, 1981–2022) 30 days before anthesis (totalizing 31 days), for the N treatments: non-fertilized (N0) and N fertilizer supply of 60 kg N ha^{-1} (N60), 100 kg N ha^{-1} (N100), and 140 kg N ha^{-1} (N140), for all five soil profiles (Table 1, Supp. Tab. S4 to S8). Since values below zero were not simulated (i.e., negative yields do not exist and are not simulated), the y-axis scale represents the range between the simulated minimum and maximum values.

grain weights from 29.7 mg to 38.2 mg, N100 from 31.3 mg to 38.3 mg, N60 from 31.8 mg to 36.6 mg, and N0, from 31.5 mg to 35.1 mg.

Analysis of variance indicated that N supply significantly affected grain number ($p < 0.001$), whereas rainfall reduction and the rainfall × N interaction were not significant ($p = 0.349$ and $p = 0.994$, respectively). For grain weight, both rainfall reduction and N supply had significant effects ($p < 0.001$), while their interaction was marginally non-significant ($p = 0.063$). Grain yield was significantly influenced by rainfall reduction, N supply, and their interaction ($p < 0.001$, Supp. Tab. S10).

4.2.3. Rainfall decreases between stem elongation and grain filling

The simulated responses of winter wheat to reduced rainfall 30 days before and after anthesis associated with different N fertilizer supply is shown in Fig. 4. In this scenario, considering all N treatments together, the means of yield, grain number and grain weight, decreased with rainfall reductions, being greatest in HS and lowest in R100. Yields went from 2.58 t ha^{-1} (R100) to 4.06 t ha^{-1} (HS), grain numbers from 7673.8 grains m^{-2} (R100) to 10,435.6 grains m^{-2} (HS), and grain weights from 32.4 mg (R100) to 37.1 mg (HS). The N0 treatment presents more similar and consistent results along the different rainfall levels than the other N treatments for grain number and yield.

As for the N treatments, the N140 had the greatest means of grain number in all rainfall levels, while for yield and grain weight, it varied. Grain numbers in N140 varied from 8642.2 grains m^{-2} (R100) to 13,353.5 grains m^{-2} (HS). In the case of the yields, the N140 had greatest mean values in HS (5.29 t ha^{-1}), R20 (5.03 t ha^{-1}), R40 (4.63 t ha^{-1}), and R60 (4.02 t ha^{-1}), while N100 had them in R80 (3.28 t ha^{-1}) and R100 (2.91 t ha^{-1}) (Supp. Tab. S11, Supp. Fig. S2). The lowest yield and grain number means were found in N0 in all rainfall levels. For grain weight in HS, similar results were found for N100 (38.3 mg) and N140 (38.2 mg), the greater values among N treatments in that rainfall level. N100 had also the greatest means in R20 (37.4 mg) and R40 (35.7 mg), while N60 had them in R60 (33.5 mg), R80 (31.9 mg) and R100 (33.4 mg). On the other hand, while the lowest mean within a rainfall level occurred in N0 for HS (35.1 mg), R20 (35.0 mg), R40 (34.3 mg), and R100 (31.1 mg), the mean of N0 (32.9 mg) was greater than N140 (32.4 mg) in R60, as well as greater (31.5 mg) than both N100 (30.9 mg) and N140 (30.1 mg) in R80.

Analysis of variance revealed that rainfall reduction, N supply, and

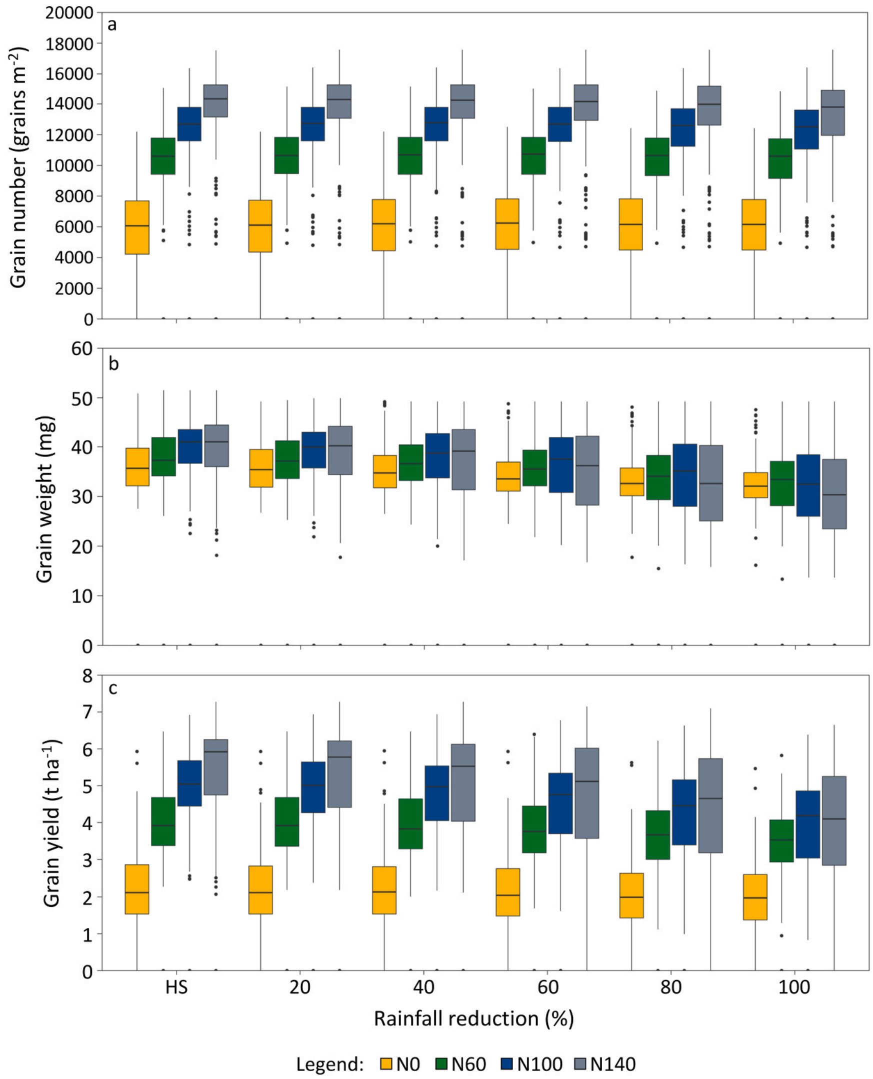

Fig. 3. Simulated responses of winter wheat to reduced rainfall 30 days after anthesis under four nitrogen fertilizer supplies. Winter wheat grain number (a), grain weight (b) and yield (c) responses to reductions of rainfall of 20 % (R20), 40 % (R40), 60 % (R60), 80 % (R80) and 100 % (R100) of the Historical Series (HS, 1981–2022) 30 days after anthesis (totalizing 31 days), for the N treatments: non-fertilized (N0) and N fertilizer supply of 60 kg N ha^{-1} (N60), 100 kg N ha^{-1} (N100), and 140 kg N ha^{-1} (N140), for all five soil profiles (Table 1, Supp. Tab. S4 to S8). Since values below zero were not simulated (i.e., negative yields do not exist and are not simulated), the y-axis scale represents the range between the simulated minimum and maximum values.

their interaction significantly affected grain number and grain yield ($p < 0.001$). For grain weight, rainfall reduction and N supply had significant effects ($p < 0.001$ and $p = 0.002$, respectively), while their interaction was not significant ($p = 0.149$, Supp. Tab. S11).

4.2.4. Rainfall decreases during the entire season

The simulated responses of winter wheat to reduced rainfall during the entire season with different N fertilizer supply is shown in Fig. 5. Considering all N treatments together, means of grain weight decreased with rainfall reductions (from 37.1 mg in HS to 23.9 mg in R100), while means of yield was the greatest in R20 (4.14 t ha^{-1}), followed by HS (4.06 t ha^{-1}), and the mean of grain number was the greatest in R40 (10,930.6 grains m^{-2}), followed by R20 (10,839.6 grains m^{-2}) and HS (10,435.6 grains m^{-2}). Also, differently than the previous scenarios, the N0 treatment presents similar and consistent results along the different rainfall levels. In some cases, under the R100 treatment, although grain weight varied between 33.6 mg and 42.2 mg (Fig. 5b), the grain number was significantly reduced (with very low values ranging from 18.0 grains m^{-2} to 20.0 grains m^{-2}, Fig. 5a). This resulted in extremely low yields, close to zero (0.006 t ha^{-1} to 0.008 t ha^{-1}, Fig. 5c), primarily due to the low grain number rather than the individual grain weight.

As for the N treatments, N140 had, generally, the greatest grain number and yield means in all rainfall levels. Grain number means went from 5500.1 grains m^{-2} (N100) to 13,353.5 grains m^{-2} (HS), while yield means went from 2.02 t ha^{-1} (R100) to 5.29 t ha^{-1} (HS). However, yield means of N140 were similar to the ones of N100 in R40, R60, R80 and R100, close to N60, and somehow to N0, in both R80 and R100 (Supp. Tab. S12, Supp. Fig. S2). The grain weights had differing outcomes. In HS, N100 and N140 presented similar results. In R20 and R100, N140 and N60 had similar results, being 36.4 mg and 36.6 mg in R20, and 23.8 mg and 23.9 mg in R100, respectively. In R40, N140 had the lowest grain weight mean (33.8 mg) and the other N treatments had similar means (either 34.3 mg or 34.4 mg). In R60, N0 had the greatest grain weight (31.4 mg), and, in R80, the means of all N treatments were similar (between 27.0 mg and 27.2 mg).

Analysis of variance revealed that rainfall reduction, N supply, and their interaction significantly affected grain number and grain yield ($p < 0.001$). For grain weight, only rainfall reduction had a significant effect ($p < 0.001$), whereas N supply and the rainfall × N interaction were not significant ($p = 0.514$ and $p = 0.875$, respectively, Supp. Tab.

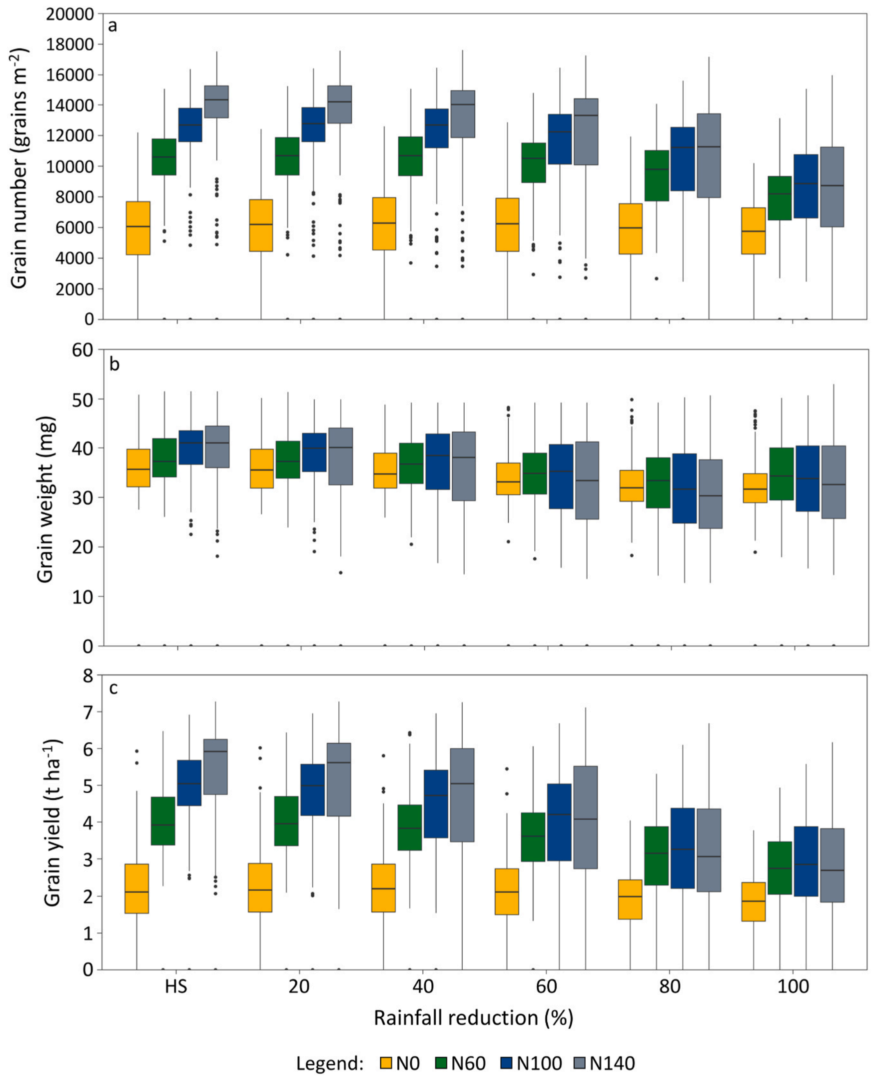

Fig. 4. Simulated responses of winter wheat to reduced rainfall 30 days before and after anthesis under four nitrogen fertilizer supplies. Winter wheat grain number (a), grain weight (b) and yield (c) responses to reductions of rainfall of 20 % (R20), 40 % (R40), 60 % (R60), 80 % (R80) and 100 % (R100) of the Historical Series (HS, 1981–2022) 30 days before and after anthesis (totalizing 61 days), for the N treatments: non-fertilized (N0) and N fertilizer supply of 60 kg N ha^{-1} (N60), 100 kg N ha^{-1} (N100), and 140 kg N ha^{-1} (N140), for all five soil profiles (Table 1, Supp. Tab. S4 to S8). Since values below zero were not simulated (i.e., negative yields do not exist and are not simulated), the y-axis scale represents the range between the simulated minimum and maximum values.

S12).

4.2.5. Principal Component analysis

Three PCAs were used to identify associations among variables (Figs. 6a to 6c). The PCAs included twelve crop and soil variables (i.e., wheat grain yield, grain number per m^2, grain weight, total aboveground biomass, grain protein content, N in grain, N in straw, plant N uptake, NHI, NUtE, LAI, and soil N leached) in two dimensions (the number of PCs selected). The PCA revealed a strong and consistent positive relationship between the yield and grain number (Fig. 6a, and Fig. 6c), which presented an even more consistent relationship with N in grain and total aboveground biomass (Figs. 6a to 6c). Yield and N leached were both negatively (Fig. 6a) and positively correlated (Fig. 6b), depending on the conditions highlighted. Also, N leached presented close relationship with NHI and NUtE (Figs. 6b and 6c), but these showed inconsistent relationships with the other variables across the figures (Figs. 6a to 6c). Grain protein showed a close association with both N in straw (Figs. 6a and 6b) and plant N uptake (Figs. 6a and 6c). Additionally, plant N uptake had a strong relationship with LAI (Fig. 6a to Fig. 6c). The contributions of the variables to PC1 and PC2 in each case, can be found in Supplementary Fig. S3. Differences between levels of N fertilizer supply, rainfall reduction and scenario of rainfall reductions were highlighted in Fig. 6a, Fig. 6b, and Fig. 6c, respectively.

In PCA with varying N fertilizer supplies (Fig. 6a), two principal components (PC1 and PC2) accounted for 92.2 % of variance for all seasons analyzed together. All variables are positively correlated to PC1, except for N leached, NUtE and NHI, which are opposed to yield-related traits (Fig. 6a). Also, the PERMANOVA analysis revealed that N supply explained 80.7 % of the variance in multivariate space ($R^2 = 0.807$, $p = 0.001$), indicating a highly significant separation between N treatments. A cluster can be seen for each N treatment, with N0 being the closest to N leached and farthest from yield, while for N140, it is the opposite. Both the N0 and N140 treatments exhibit the greatest variability, whether in relation to PC1 (horizontally) or PC2 (vertically).

In the PCA focused on levels of rainfall reduction (Fig. 6b), PC1 and PC2 explained 80.85 % of the variance for all seasons combined. All variables positively correlated with PC1 (Fig. 6b). The R100 data generally positioned further from yield, whereas HS was closer, indicating more favorable outcomes under actual conditions. Rainfall reduction treatments significantly influenced the multivariate distribution of samples, explaining 41.9 % of the total variance ($R^2 = 0.419$, $p = 0.001$). However, sample clustering was only partial, with

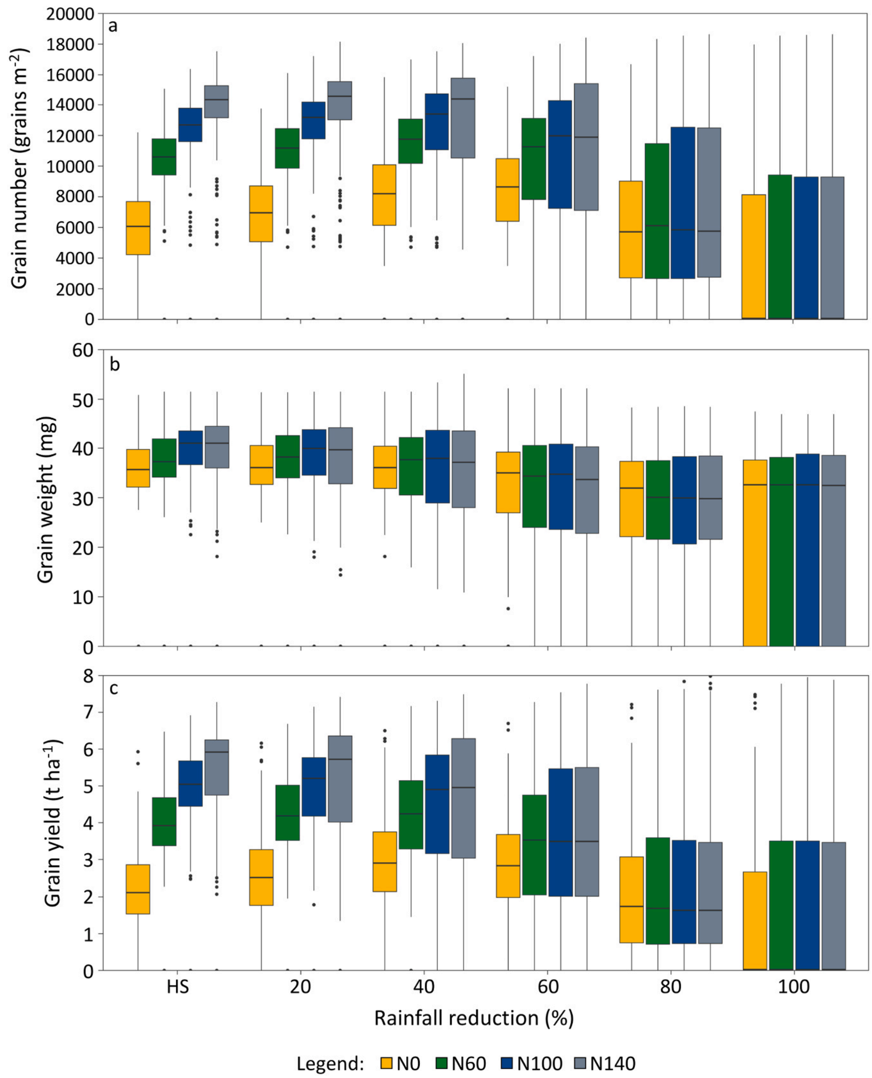

Fig. 5. Simulated responses of winter wheat to reduced rainfall during the entire season under four nitrogen fertilizer supplies. Winter wheat grain number (a), grain weight (b) and yield (c) responses to reductions of rainfall of 20 % (R20), 40 % (R40), 60 % (R60), 80 % (R80) and 100 % (R100) of the Historical Series (HS, 1981–2022) from sowing to July 31st, for the N treatments: non-fertilized (N0) and N fertilizer supply of 60 kg N ha^{-1} (N60), 100 kg N ha^{-1} (N100), and 140 kg N ha^{-1} (N140), for all five soil profiles (Table 1, Supp. Tab. S4 to S8). Since values below zero were not simulated (i.e., negative yields do not exist and are not simulated), the y-axis scale represents the range between the simulated minimum and maximum values.

noticeable overlap between rainfall treatments in PCA space (Fig. 6b). Specifically, in the R60 treatment (green points in Fig. 6b), the analysis revealed higher N uptake and grain N content compared to other rainfall treatments, although this did not translate into yield changes relative to other treatments. The R80 and, particularly, the R100 treatments exhibited the greatest variability in points concerning PC1 and PC2, showing that other factors such as soil characteristics, N supply, and timing of water stress become more influential on the growth and N variables of wheat in these conditions.

The two principal components accounted for 84.59 % of the variance for all seasons analyzed together when focusing on the different scenarios of rainfall reductions (Fig. 6c). All variables demonstrated a positive correlation with PC1 (Fig. 6c). The PERMANOVA analysis showed that the scenario factor explained 24.8 % of the variance in multivariate space ($R^2 = 0.248$, $p = 0.001$), thus a statistically significant but moderate separation between scenarios. As anticipated, the scenarios of rainfall reduction exclusively around anthesis exhibited similar characteristics due to their overlapping conditions. Notably, grain number and grain weight were the variables most strongly correlated with grain yield. The greatest variability in points relative to both PC1 and PC2 only occurred when the rainfall reduction occurred during the entire season.

5. Discussion

Our study systematically assessed the interaction between phased rainfall reduction and N management across five different Cambisols, using 42 years of climatic data to ensure a robust evaluation of winter wheat resilience under Swiss conditions. By integrating multiple factors (rainfall reductions, timing of these reductions, and N supply) the study provides a comprehensive framework for understanding crop responses to future climate scenarios with reduced rainfall.

5.1. Calibration and evaluation of the DSSAT-Nwheat

The calibration and validation of the DSSAT-Nwheat model for the genotype CH Nara demonstrated its capacity to accurately simulate key crop variables, particularly phenological stages, such as anthesis and maturity dates. The high accuracy and precision achieved during this phase suggest that the model effectively captured the main drivers of

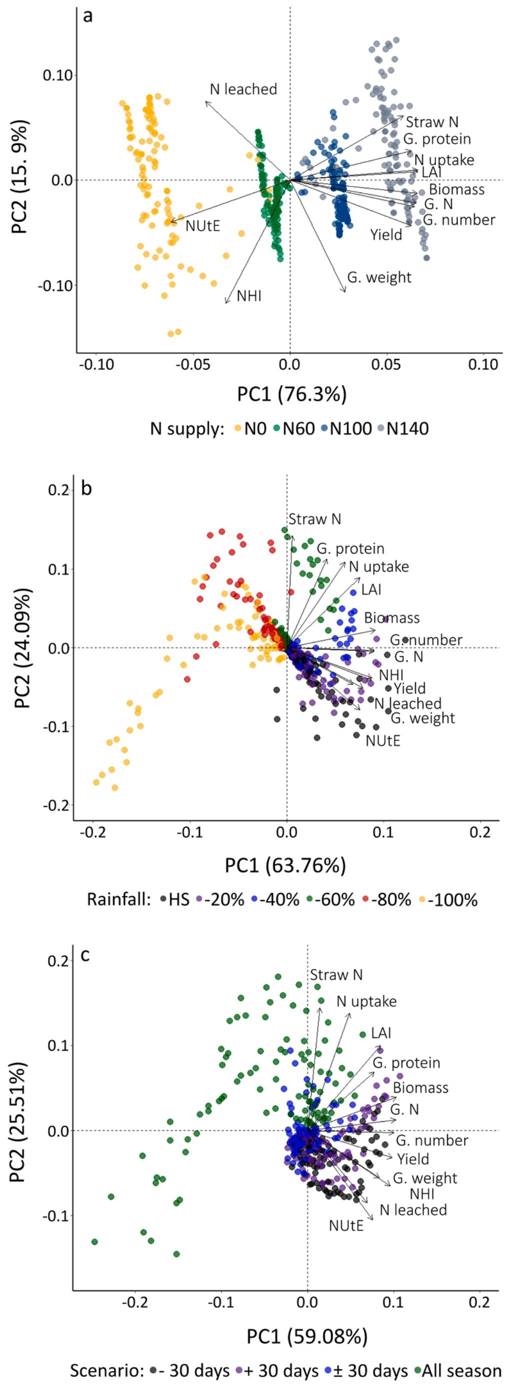

Fig. 6. Principal Component analysis (PCA) of simulated winter wheat production variables. The figure contains the first two principal components, PC1 and PC2, and their respective scores explaining variation within the data of all seasons analyzed together, focused on N fertilizer supply (**a**), rainfall reduction (**b**), and scenario of rainfall reductions (**c**). Arrows indicate the strength of the trait influence on the first two PCs. Factors included wheat grain yield (Yield), grain number per m^2 (G. number), grain weight (G. weight), total aboveground biomass (Biomass), grain protein content (G. protein), grain N (G. N), straw N, plant N uptake (N uptake), N harvest index (NHI), N utilization efficiency (NUtE), leaf area index (LAI), soil N leached (N leached).

crop development, such as temperature and solar radiation responses. Similar results for phenology in wheat calibration were found by Shoukat et al. (2024) and Liu et al. (2020), applying two (DSSAT CROPSIM-CERES and DSSAT-Nwheat) and three (CERES-Wheat included) models, respectively. Simulations of other variables, such as grain yield and grain number, showed a lower, but still acceptable level of accuracy and precision. Ye et al. (2020) applying DSSAT-Nwheat, also found a RMSE for winter wheat grain yield in China of 1.1 t ha^{-1} in model evaluation. However, this could also reflect the high volume of rainfall that often occurs in the region of the field trials used in our study (Fig. 1), and its potential for waterlogging, which is not yet fully reflected in the model's structure (Nóia Júnior et al., 2023b). Although some studies have indicated the inclusion of a waterlogging module in DSSAT-Nwheat, considering the effects of waterlogging on root activity and leaf area index (LAI) (Shelia et al., 2019), or on photosynthesis, growth, transpiration, biomass partitioning, and phenology (Nóia Júnior et al., 2023a), these versions of DSSAT-Nwheat with waterlogging module are still not available for download via the DSSAT platform website. The version of DSSAT-Nwheat used in this study does not account for the negative impacts of waterlogging on wheat growth, potentially leading to overestimations in simulated yields compared to observed values during seasons with excess water, as observed in this study.

Additionally, while the use of field trials in the same location and under mainly similar weather conditions might be viewed as a limitation for model calibration, the inclusion of three contrasting seasons, one of which includes a field representation of the projected reduction in rainfall (with rainout shelters), along with five soil profiles, provides sufficient variability for an effective calibration process. According to He et al. (2017), calibrating a CM with data from contrasting seasons (which was represented by different sowing dates in their study) can reduce the error or uncertainty to minimum, while calibrating it with one or multiple similar seasons often leads to equifinality, resulting in high uncertainty in the simulation outcomes. Although this study used a single model for calibration, which may limit performance, CMs inherently involve various uncertainties due to the complexity of their systems (Battisti, 2016; Wang et al., 2017), the number of parameters requiring calibration, and the extensive input data needed (Duarte, 2018). To further reduce these uncertainties, future studies could consider the use of a multi-model ensemble approach, which tends to outperform individual models in terms of accuracy (Asseng et al., 2013; Bassu et al., 2014; Battisti et al., 2017). In general, while the calibration and evaluation in this study achieved adequate accuracy, incorporating experimental data from a wider range of genotypes and climatic conditions, along with a multi-model ensemble approach, could further enhance the precision and robustness of simulations for more complex variables.

5.2. Winter wheat sensitivity to rainfall decrease during stem elongation and N compensation

Greater reductions in rainfall (>60 %) during stem elongation (scenario anthesis minus 30 days) led to a significant decrease compared to HS in both grain number (up to 21 %) and yield (up to 20 %), reflecting the critical importance of water availability during early crop development. This is in line with previous experimental studies emphasizing water as a limiting factor in determining yield potential during early growth stages (Brisson et al., 2010; Liu et al., 2016). Liu et al. (2016) reported that a drought-resistant winter wheat genotype showed greater yields under mild drought conditions (80 mm of irrigation) during the reviving-jointing, jointing-anthesis, and grain filling stages, and lower under moderate (60 mm) and severe drought (40 mm) across all stages. On the other hand, N fertilizer showed a compensatory effect by maintaining similar levels of both grain number and yield in different reduced rainfall conditions during stem elongation. This aligns with other studies, in which N supply was able to alleviate the effects of drought stress, on crop growth and development (Zhang et al., 2008; Xiong et al., 2018; Moghaddam et al., 2023; Ru et al., 2023). Grain weight was found to be greatest under HS and in R100 conditions compared to other rainfall scenarios. Across all rainfall treatments, grain weight was consistently higher at the N100 level, except in R100, and lowest in N0.

These results indicate that under actual conditions, the crop was able to achieve higher grain weight when sufficient N fertilizer was applied, supporting the role of N in enhancing yield under actual weather patterns.

5.3. Limited yield impacts of rainfall reductions from anthesis to grain filling

In the end of flowering and grain filling scenario (scenario anthesis plus 30 days), both grain weight and yield decreased with rainfall reductions, with just a reduction up to −40 % of rainfall (from 4.06 t ha^{-1} to 3.90 t ha^{-1}), consistent with findings that post-anthesis water restriction can have major effects on grain yield (Gevrek and Atasoy, 2012; Liu et al., 2016; Mohammadi, 2024). This is also in agreement with experimental findings of Bongiovani et al. (2024), in which reductions of up to 40 % of rainfall during grain filling did not affect yield compared to rainfed conditions. Grain number was higher in the moderate rainfall reduction scenarios (R20 and R40) compared to HS, suggesting that a slight reduction in rainfall in the region might foster better nutrient use efficiency, which could result in higher grain numbers. Yield and grain number were greatest in the N140 treatment, while the lowest values were observed at N0, reaffirming the importance of adequate N fertilization for attaining greater yields. This was also demonstrated by Wang et al. (2023). Interestingly, grain weight was lowest in R100 across all N treatments, while it peaked in the HS scenario.

5.4. Rainfall reduction across phenological stages intensifies yield losses despite N input

Rainfall reductions between stem elongation and grain filling (scenario anthesis ±30 days) consistently led to a decrease in grain weight, grain number, and yield, highlighting the overarching importance of adequate water availability throughout the reproductive crop phase. This corroborates with results of Liu et al. (2016). Similarly, Qaseem et al. (2019) obtained reductions in grain yield (-44.66 %) and yield components (including grain number), by imposing a drought stress of 30 % of field capacity, from heading to maturity of 180 elite wheat genotypes. Grain number was highest in the N140 treatment and lowest in N0, with similar trends observed for yield, which suggests that N fertilization plays a crucial role in mitigating the negative effects of water stress. Adequate N supply could alleviate drought stress on wheat (Ru et al., 2023), by boosting plant growth and biomass accumulation (Agami et al., 2018). Also, the similar performance of N140 and N100 suggests that under certain conditions, including HS, it may be possible to reduce N application without significant yield losses, making it more sustainable and cost-effective. These findings have important implications not only for optimizing fertilizer use in rainfall-limited environments, but also in Swiss wheat production, in which 140 kg N ha^{-1} is recommended as input (PRIF, Sinaj et al., 2017).

5.5. Extended water limitation emphasizes the need for N use optimization

When analyzing the entire season scenario, grain weight consistently decreased with reduced rainfall. However, yield and grain number were higher in the R20 and R40 scenarios compared to HS. This suggests that this particular drought tolerant winter wheat genotype (Touzy et al., 2019) may be adapted to slightly drier environments than the studied region, with potential to benefit from the 40 % projected rainfall decrease (CH2018, 2018). On the other hand, even under severely limited rainfall, wheat could sustain yield if it effectively accesses and conserves soil water. In a study by Angus et al. (1980), wheat grown with only 50 mm of in-season rainfall in a subtropical environment achieved grain yields of up to 3 t ha^{-1} by relying on stored soil moisture from the previous summer and by extracting deep soil water gradually to maintain moisture for the grain-filling phase. Also, the high capacity of CH Nara to allocate the accumulated N to the grains (Caldelas et al., 2023; Bongiovani et al., 2024), could improve its response to moderate drought conditions, by reallocating resources more efficiently. Additionally, although more extreme than the actual climate projections for the region (CH2018, 2018), the similar results across N140, N100, and N60 indicate a potential opportunity to reduce N fertilizer use without compromising yield. Reduced N applications in N100, and N60 treatments achieved yields equivalent to higher N levels (N140), indicates that minimizing N use could decrease agricultural costs and mitigate environmental degradation. This finding corroborates Zörb et al. (2018), highlighting the ecological advantages of curbing excessive fertilization. However, it is important to note that the present study primarily considered rainfall reduction as the climate stressor. The effects of increasing temperatures and CO_2 concentration, both of which are expected under future climate scenarios, were not directly incorporated into the simulations. Elevated temperatures can enhance N losses through volatilization and other processes, potentially requiring higher, not lower, N applications to maintain yield stability (Drame et al., 2023; Wang et al., 2021). Rising atmospheric CO_2 concentrations can impair key physiological processes of N uptake and assimilation in C_3 plants, such as wheat, reducing tissue N content and potentially limiting NUE (Gojon et al., 2023). Thus, while the results suggest opportunities for N reduction under rainfall-limited conditions, future studies should integrate not only temperature and rainfall changes but also elevated CO_2 effects to better refine N management recommendations.

In the absence of N supply (N0), wheat yields were unaffected by rainfall variations during grain filling or anthesis. However, when rainfall reductions occurred throughout the entire season, the R20, R40, and R60 treatments resulted in yield increases of 16 % (2.6 t ha^{-1}), 33 % (2.9 t ha^{-1}), and 26 % (2.8 t ha^{-1}), respectively, compared to the actual scenario (HS), which yielded 2.2 t ha^{-1}.

5.6. Key relationships between wheat and soil variables influenced by N and water availability

The results from the PCA analysis reveal key associations between crop and soil variables under different conditions. Across all four PCAs, strong positive relationships were identified, particularly between wheat grain yield, grain number, grain N and total aboveground biomass. This is consistent with the studies of Fischer (2011), Pedro et al. (2012), and Bongiovani et al. (2024). Bongiovani et al. (2024) found that grain number per m^2 was more closely related to grain yield, which was highlighted by the genotype Cellule, of intermediate drought tolerance, while the genotype CH Nara (drought tolerant) had greater protein content in grains, thus higher grain N content. Nevertheless, Golba et al. (2018) found that in a warm-summer humid continental climate, the number of ears per m^2 is the key factor for achieving high grain yields.

Grain protein content, a crucial factor for farmer financial compensation in Swiss bread wheat production (Swiss granum, 2020), demonstrated strong correlations with N in straw and plant N uptake, highlighting that increased N uptake significantly enhances protein levels (Figs. 6a to 6c). Furthermore, plant N uptake was positively associated with LAI across all PCA analyses, underlining the role of N in fostering canopy development and biomass, where higher N levels are tied to enhanced LAI and vegetative growth (Bali et al., 1991; Rahman et al., 2014). However, excessive N can lead to increased water consumption due to greater canopy transpiration without yielding benefits, as suggested by Steduto et al. (2012). This pattern is evident in our findings, for instance, in the R60 treatment (60 % rainfall reduction), where higher N uptake and grain N content, comparable to other rainfall reductions levels, did not translate into higher yields (Fig. 6b). This indicates that excessive N application does not necessarily result in yield increases, particularly under conditions of high rainfall, common during the Swiss wheat growing season (Fig. 1), where even significant reductions in rainfall during key phenological stages do not necessarily impact productivity adversely.

The PCA analysis also indicates the contrasting relationship between yield and N leached, being both negative (Fig. 6a) and positively correlated (Fig. 6b), depending on what treatment was highlighted. This shows that, at this location, environmental factors influence differently the trade-off between N efficiency and crop productivity. Their negative correlation was found when different N supplies (Fig. 6a) were evidenced, with yield being more associated with higher N supplies, while N leached, with lower N. On the other hand, their positive correlation was found when rainfall reductions were evidenced, notably in conditions closer to HS, of more rainfall (HS and R20; Fig. 6b). Another relationship found particularly under higher rainfall conditions (HS and R20; Fig. 6b) was between N leached and both NHI and NUtE, as well as under conditions of shorter durations of rainfall reduction (30 days before anthesis and 30 days after anthesis; Fig. 6c). This suggests that under mild reductions in rainfall, although N leaching is still likely to occur due to the naturally high annual precipitation of the location (Fig. 1), the plant's ability to accumulate N and efficiently remobilize it to the grain may remain largely unaffected. This is especially relevant given that wheat accumulates most of its N before anthesis, which is subsequently remobilized to the grain during grain filling for protein synthesis (Triboi and Triboi-Blondel, 2002; Kong et al., 2016). Beyond this, no other consistent relationships between NHI and NUtE and the studied variables were observed in this analysis.

The impact of varying N fertilizer supply and reduced rainfall on these relationships was also evident. For instance, the PCA analysis with highlighted N treatments reveals distinct clusters for different N levels (Fig. 6a), with N100 and N140 displaying some overlapping points, which were also identified in previous yield analysis (Supp. Tab. S11 and S12, Supp. Fig. S2). This supports the findings of Levy et al. (2007) in Switzerland, in which varying N doses (65 kg N ha^{-1}, 105 kg N ha^{-1}, 145 kg N ha^{-1}, and 185 kg N ha^{-1}) were applied. They reported that the marginal gains in both yield and quality decline with each incremental increase in N fertilization (Levy et al., 2007). In contrast, rainfall reductions had more variable effects, with rainfall treatments producing less defined clusters, reflecting similarities in response. Thus, the PCAs provided insights into how these variables interact under different agronomic and environmental conditions.

This study investigates the relationship between N use and varying rainfall conditions in Swiss wheat production. Employing the DSSAT-Nwheat model calibrated for a wheat production region using rainout shelters experiments to control rainfall, the study demonstrates that wheat yields remain stable under up to 40 % rainfall reduction across different N application rates and timings. However, when rainfall reductions exceed 60 %, particularly at N levels above 100 kg ha^{-1}, significant yield decreases are observed. While the optimal yield was achieved at 140 kg N ha^{-1}, the effectiveness of this N rate declined under scenarios of reduced rainfall, suggesting that N guidelines might need adjustment in anticipation of future climatic changes. This research is important for tailoring N management to optimize winter wheat production in the face of climate change, as also suggested by Martre et al. (2024).

Some limitations of this study must be acknowledged. First, the calibration was based on a 4-year field dataset, which, although incorporating seasonal variability, remains relatively short when compared to the 42 years of simulation period. Extrapolating from a limited calibration period can introduce uncertainties, particularly regarding processes influenced by long-term soil and climatic variability. Second, some soil parameters were empirically estimated, and the DSSAT-Nwheat version used does not simulate the effects of waterlogging (Nóia Júnior et al., 2023b), which may have influenced yield simulations under wetter conditions. Future work should focus on expanding the field dataset across more years and varying climatic conditions, and on integrating updated model versions that include waterlogging responses.

6. Conclusions

This study systematically integrated multiple sources of variation (rainfall reduction timing and magnitude, N management, and soil diversity) using a robust long-term dataset, providing a solid framework for evaluating wheat resilience strategies under climate change. Our simulations indicated that a rainfall reduction of up to 40 % (as currently projected for Switzerland; CH2018, 2018) did not significantly affect wheat yields, regardless of N rate or phenological. A substantial negative impact on yield was only observed with rainfall reductions of over 60 % throughout the entire cropping season, demonstrating considerable resilience of CH Nara genotype to reduced rainfall.

In treatments where N fertilizer application exceeded 100 kg ha^{-1}, yield reductions occurred with rainfall declines as low as 20 % and were more pronounced under reductions above 60 %. These effects were independent of the phenological stage during which the rainfall reduction occurred, highlighting greater yield sensitivity when N applications exceed 100 kg ha^{-1} in Switzerland.

Under current rainfall scenarios (i.e., simulations based on the historical rainfall patterns from 1981 to 2022), the highest yields were obtained with 140 kg N ha^{-1}. However, under future scenarios with reduced rainfall, the yield advantage over 100 kg N ha^{-1} diminished. This suggests that under drier conditions, the current N rate recommendation for Swiss wheat farmers (140 kg N ha^{-1}; PRIF, Sinaj et al., 2017) could be revised and potentially reduced, especially when considering resilience to climate variability. Furthermore, grain number per m^2 emerged as a critical factor in ensuring grain yields under varying N supply and rainfall conditions in Switzerland. While this study focused mainly on grain yield, further studies of Swiss wheat production should also assess grain quality and environmental consequences.

A key limitation of this study is the exclusion of projected increases in temperature and CO_2, which could significantly influence N dynamics. Higher temperatures could exacerbate N losses, and elevated CO_2 could reduce plant N uptake and efficiency, both potentially offsetting benefits of reduced fertilizer inputs. Future research should therefore integrate rainfall, temperature and CO_2 projections to develop more comprehensive N management strategies under climate change. Additionally, broader field validation across years and environments, as well as inclusion of other climatic stressors like heat and waterlogging, is essential to refine recommendations and better support wheat production in increasingly variable climates.

CRediT authorship contribution statement

Paola de Figueiredo Bongiovani: Writing – review & editing, Writing – original draft, Visualization, Validation, Methodology, Investigation, Formal analysis, Data curation, Conceptualization. **Amanda Burton:** Writing – review & editing, Writing – original draft, Methodology, Investigation, Conceptualization. **Lilia Levy Häner:** Writing – review & editing, Writing – original draft, Resources, Methodology. **Senthold Asseng:** Writing – review & editing, Writing – original draft, Visualization, Validation, Supervision, Methodology, Conceptualization. **Juan Manuel Herrera:** Writing – review & editing, Writing – original draft, Supervision, Resources, Methodology, Conceptualization. **Emmanuel Frossard:** Writing – review & editing, Writing – original draft, Validation, Supervision, Methodology, Conceptualization. **Rogério de S. Nóia Júnior:** Writing – review & editing, Writing – original draft, Visualization, Methodology, Investigation, Formal analysis, Conceptualization. **Diego N. L. Pequeno:** Writing – review & editing, Writing – original draft, Methodology, Investigation, Data curation, Conceptualization.

Declaration of Competing Interest

The authors declare the following financial interests/personal relationships which may be considered as potential competing interests.

Appendix A. Supporting information

Supplementary data associated with this article can be found in the online version at doi:10.1016/j.eja.2025.127728.

Data Availability

Data will be made available on request.

References

Agami, R.A., Alamri, S.A.M., Abd El-Mageed, T.A., Abousekken, M.S.M., Hashem, M., 2018. Role of exogenous nitrogen supply in alleviating the deficit irrigation stress in wheat plants. Agric. Water Manag 210, 216–270. https://doi.org/10.1016/j.agwat.2018.08.034.

Angus, J.F., Nix, H.A., Russell, J.S., Kruizinga, J.E., 1980. Water use, growth and yield of wheat in a subtropical environment. Aust. J. Agric. Res. 31, 873–876.

ARVALIS, 2025. Les fiches ARVALIS. http://www.fiches.arvalis-infos.fr. Accessed 15 January 2025.

Asseng, S., Keating, B.A., Fillery, I.R.P., Gregory, P.J., Bowden, J.W., Turner, N.C., Palta, J.A., Abrecht, D.G., 1998. Performance of the APSIM-wheat model in western Australia? Field Crops Res 57 (2), 163–179. https://doi.org/10.1016/S0378-4290(97)00117-2.

Asseng, S., McIntosh, P.C., Wang, G., Khimashia, N., 2012. Optimal N fertiliser management based on a seasonal forecast. Eur. J. Agron. 48, 66–73. https://doi.org/10.1016/j.eja.2011.12.005.

Asseng, S., Ewert, F., Rosenzweig, C.J.W., Hatfield, J.L., Ruane, A.C., Bootle, K.J., Thorburn, P.J., Rotter, R.P., Cammarano, D., Brisson, N., Basso, B., Matre, P., Aggarwal, P.K., Angulo, C., Bertuzzi, P., Biernath, C., Challinor, A.J., Doltra, J., Gayler, S., Goldberg, R., Grant, R., Heing, L., Hooker, J., Hunt, L.A., Ingwersen, J., Izaurralde, R.C., Kersebaum, K.C., Muller, C., Naresh Kumar, S., Nendel, C., O'leary, G., Olesen, J.A., Osborne, T.M., Palosuo, T., Stockle, C., Stratonovitch, P., Streck, T., Supit, I., Tao, F., Travasso, M., Waha, K., Wallach, D., White, J.W., Williams, J.R., Wolf, J., 2013. Uncertainty in simulation wheat yields under climate change. Nat. Clim. Change 3, 827–832.

Bali, S.A., Khan, G.M., Shah, M.H., Singh, K.N., Singh, T., 1991. Yield behaviour and various physioagronomic characters of wheat (*Triticum aestivum*) and triticale genotypes as influenced by nitrogen fertilization under the temperate conditions of Kashmir. Indian J. Agron. 36, 482–487.

Bassu, S., Brisson, N., Durand, J.L., Boote, K., Lizaso, J., Jones, J.W., Rosenzweig, C., Ruane, A.C., Adam, M., Baron, C., Basso, B., Biernath, C., Boogaard, H., Conijn, S., Corbeels, M., Deryng, D., De Sanctis, G., Gayler, S., Grassini, P., Hatfield, J., Hoek, S., Izaurralde, C., Jongschaap, R., Kemanian, A.R., Kersebaum, K.C., Kim, S.H., Kumar, N.S., Makowski, D., Müller, C., Nendel, C., Priesack, E., Pravia, M.V., Sau, F., Shcherbak, I., Tao, F., Teixeira, E., Timlin, D., Waha, K., 2014. How do various maize crop models vary in their responses to climate change factors? Glob. Change Biol. Oxf. 20, 2301–2320.

Battisti, R., 2016. Calibration, uncertainties and use of soybean crop simulation models for evaluating strategies to mitigate the effects of climate change in Southern Brazil [Doctoral dissertation, University of São Paulo]. ⟨https://www.teses.usp.br/teses/disponiveis/11/11152/tde-03102016-162340/en.php⟩.

Battisti, R., Sentelhas, P.C., Boote, K.J., 2017. Inter-comparison of performance of soybean crop simulation models and their ensemble in southern Brazil. Field Crops Res. Amst. 200, 28–37.

Beck, H., Zimmermann, N., McVicar, T., Vergopolan, N., Berg, A., Wood, E.F., 2018. Present and future Köppen-Geiger climate classification maps at 1-km resolution. Sci. Data 5, 180214. https://doi.org/10.1038/sdata.2018.214.

Bongiovani, P., de, F., Frossard, E., Nóia Júnior, R., de, S., Asseng, S., Vuille-dit-Buille, N., Burton, A., Herrera, J.M., 2024. Responses of winter wheat genotypes to reduced rainfall, nitrogen fertilization and pre-crops in Switzerland. Field Crop. Res. 308, 109272. https://doi.org/10.1016/j.fcr.2024.109272.

Brabant, C., Levy Häner, L., 2016. Influ. De. la fumure azotée Et. De. Son. -fractionnement sur la Qual. é Boulang. ère du Bl. é. Rech. Agron. Suisse 7 (2), 88–97.

Brisson, N., Gate, P., Gouache, D., Charmet, G., Oury, F.-X., Huard, F., 2010. Why are wheat yields stagnating in Europe? a comprehensive data analysis for France. Field Crop. Res. 119, 201–212. https://doi.org/10.1016/j.fcr.2010.07.012.

Burton, A., Levy Häner, L., Schaad, N., Strebel, S., Vuille-dit-Bille, N., Bongiovani, P.B., Holzkämper, A., Pellet, D., Herrera, J., 2024. Evaluating nitrogen fertilization strategies to optimize yield and protein in top winter wheat varieties across Switzerland. Field Crop. Res. 307, 109251. https://doi.org/10.1016/j.fcr.2024.109251.

Caldelas, C., Rezzouk, F.Z., Gutiérrez, N.A., Diez-Fraile, M.C., Ortega, J.L.A., 2023. Interaction of genotype, water availability, and nitrogen fertilization on the mineral content of wheat grain. Food Chem. 404, 134565. https://doi.org/10.1016/j.foodchem.2022.134565.

CH2018, 2018. CH2018 – Climate Scenarios for Switzerland. National Centre for Climate Services, Zurich, Switzerland.

R. Core Team, 2024. R: A language and environment for statistical computing. R Foundation for Statistical Computing: Vienna, Austria.

Drame, M., Carswell, A., Roberts, W., Hood, J., Jemo, M., Heuer, S., Kirk, G., Pawlett, M., Misselbrook, T., 2023. Effects of hotter, drier conditions on gaseous losses from nitrogen fertilisers. J. Environ. Manag. 345, 118671. https://doi.org/10.1016/j.jenvman.2023.118671.

Duarte, Y.C.N., 2018. Modelos de simulação da cultura do milho: uso na determinação das quebras de produtividade (Yield Gaps) e na previsão de safra da cultura no Brasil [Master's thesis, University of São Paulo]. ⟨https://teses.usp.br/teses/disponiveis/11/11152/tde-15052018-104958/pt-br.php⟩.

Duarte, Y.C.N., Sentelhas, P.C., 2020. Intercomparison and performance of maize crop models and their ensemble for yield simulations in Brazil. Int. J. Plant Prod. 14, 127–139. https://doi.org/10.1007/s42106-019-00073-5.

EU Commission, 1991. Directive 91/676/EEC. Council Directive of 12 December 1991 concerning the protection of waters against pollution caused by nitrates from agricultural sources. Off. J. Eur. Community L375, 1–8.

FAOSTAT, 2022. FAO Statistics Division. Food and Agriculture Organization of the United Nations.

Finger, R., Schmid, S., 2008. Modeling agricultural production risk and the adaptation to climate change. Agric. Financ. Rev. 68 (1), 25–41.

Fischer, A.M., Strassmann, K.M., Croci-Maspoli, M., Hama, A.M., Knutti, R., Kotlarski, S., Schär, C., Schnadt Poberaj, C., Ban, N., Bavay, M., Beyerle, U., Bresch, D.N., Brönnimann, S., Burlando, P., Casanueva, A., Fatichi, S., Feigenwinter, I., Fischer, E. M., Hirschi, M., Liniger, M.A., Marty, C., Medhaug, I., Peleg, N., Pickl, M., Raible, C. C., Rajczak, J., Rössler, O., Scherrer, S.C., Schwierz, C., Seneviratne, S.I., Skelton, M., Sørland, S.L., Spirig, C., Tschurr, F., Zeder, J., Zubler, E.M., 2022. Climate Scenarios for Switzerland CH2018 - Approach and Implications. Climate Services 26, 100288, ISSN 2405-8807. https://doi.org/10.1016/j.cliser.2022.100288.

Fischer, R.A., 2011. Wheat physiology: a review of recent developments. Crop Pasture Sci. 62, 95–114.

Fuhrer, J., Beniston, M., Fischlin, A., Frei, C., Goyette, S., Jasper, K., Pfister, C., 2006. Climate risks and their impact on agriculture and forests in Switzerland. Climate Variability, Predictability and Climate Risks. Springer, pp. 79–102.

Gevrek, M.N., Atasoy, G.D., 2012. Effect of post anthesis drought on certain agronomical characteristics of wheat under two different nitrogen application conditions. Turk. J. Field Crops 17 (1), 19–23.

Gojon, A., Cassan, O., Bach, L., Lejay, L., Martin, A., 2023. The decline of plant mineral nutrition under rising CO_2: Physiological and molecular aspects of a bad deal. Trends Plant Sci. 28 (2), 185–198. https://doi.org/10.1016/j.tplants.2022.09.002.

Golba, J., Studnicki, M., Gozdowski, D., Mądry, W., Rozbicki, J., 2018. Influence of genotype, crop management, and environment on winter wheat grain yield determination based on components of yield. Crop Sci. 58, 660–669. https://doi.org/10.2135/cropsci2017.07.0425.

He, D., Wang, E., Wang, J., Robertson, M.J., 2017. Data requirement for effective calibration of process-based crop models. Agric. For. Meteorol. 234235 136–148. https://doi.org/10.1016/j.agrformet.2016.12.015.

Holzworth, D.P., Huth, N.I., deVoil, P.G., Zurcher, E.J., Herrmann, N.I., McLean, G., Chenu, K., van Oosterom, E.J., Snow, V., Murphy, C., Moore, A.D., Brown, H., Whish, J.P.M., Verrall, S., Fainges, J., Bell, L.W., Peake, A.S., Poulton, P.L., Hochman, Z., Thorburn, P.J., Gaydon, D.S., Dalgliesh, N.P., Rodriguez, D., Cox, H., Chapman, S., Doherty, A., Teixeira, E., Sharp, J., Cichota, R., Vogeler, I., Li, F.Y., Wang, E., Hammer, G.L., Robertson, M.J., Dimes, J.P., Whitbread, A.M., Hunt, J., van Rees, H., McClelland, T., Carberry, P.S., Hargreaves, J.N.G., MacLeod, N., McDonald, C., Harsdorf, J., Wedgwood, S., Keating, B.A., 2014. APSIM – evolution towards a new generation of agricultural systems simulation. Environ. Model. Softw. 62, 327–350. https://doi.org/10.1016/j.envsoft.2014.07.009.

Hoogenboom, G., Porter, C.H., Boote, K.J., Shelia, V., Wilkens, P.W., Singh, U., White, J. W., Asseng, S., Lizaso, J.I., Moreno, L.P., Pavan, W., Ogoshi, R., Hunt, L.A., Tsuji, G. Y., Jones, J.W., 2019. The DSSAT crop modeling ecosystem. In: p. 173–216 [K.J. Boote, editor] Advances in Crop Modeling for a Sustainable Agriculture. Burleigh Dodds Science Publishing, Cambridge, United Kingdom. https://doi.org/10.19103/AS.2019.0061.10.

Hoogenboom, G., C.H. Porter, V. Shelia, K.J. Boote, U. Singh, W. Pavan, F.A.A. Oliveira, L.P. Moreno-Cadena, T.B. Ferreira, J.W. White, J.I. Lizaso, D.N.L. Pequeno, B.A. Kimball, P.D. Alderman, K.R. Thorp, S.V. Cuadra, M.S. Vianna, F.J. Villalobos, W.D. Batchelor, S. Asseng, M.R. Jones, A. Hopf, H.B. Dias, L.A. Hunt, and J.W. Jones., 2024. Decision Support System for Agrotechnology Transfer (DSSAT) Version 4.8.2.000 (www.DSSAT.net). DSSAT Foundation, Gainesville, Florida, USA.

HuntL.A.; Boote, K.J., 1998. Data for model operation, calibration, and evaluation. In: Tsuji, G.Y.; Hoogenboom, G.; Thornton, P.K., 1998. Understanding options for agricultural production. Dordrecht: Kluwer Ac. Pub., ch. 2, 9–40.

Jägermeyr, J., Müller, C., Ruane, A.C., Elliott, J., Balkovic, J., Castillo, O., Faye, B., Foster, I., Folberth, C., Franke, J.A., Fuchs, K., Guarin, J.R., Heinke, J., Hoogenboom, G., Iizumi, T., Jain, A.K., Kelly, D., Khabarov, N., Lange, S., Lin, T.-S., Liu, W., Mialyk, O., Minoli, S., Moyer, E.J., Okada, M., Phillips, M., Porter, C., Rabin, S.S., Scheer, C., Schneider, J.M., Schyns, J.F., Skalsky, R., Smerald, A., Stella, T., Stephens, H., Webber, H., Zabel, F., Rosenzweig, C., 2021. Climate impacts on global agriculture emerge earlier in new generation of climate and crop models. Nat. Food 2, 873–885. https://doi.org/10.1038/s43016-021-00400-y.

Ji, X., Shiran, B., Wan, J., Lewis, D.C., Jenkins, C.L.D., Condon, A.G., Richards, R.A., Dolferus, R., 2010. Importance of pre-anthesis anther sink strength for maintenance of grain number during reproductive stage water stress in wheat. Plant Cell Environ. 33, 926–942. https://doi.org/10.1111/j.1365-3040.2010.02130.x.

Jones, J.W., Hoogenboom, G., Porter, C.H., Boote, K.J., Batchelor, W.D., Hunt, L.A., Wilkens, P.W., Singh, U., Gijsman, A.J., Ritchie, J.T., 2003. The DSSAT cropping system model. Eur. J. Agron. 18, 235–265. https://doi.org/10.1016/S1161-0301(02)00107-7.

Kassie, B.T., Asseng, S., Porter, C.H., Royce, F.S., 2016. Performance of DSSAT-Nwheat across a wide range of current and future growing conditions. Eur. J. Agron. 81, 27–36. https://doi.org/10.1016/j.eja.2016.08.012.

Kim, Y.-U., Webber, H., Adiku, S.G.K., Nóia Júnior, R., de, S., Deswarte, J.-C., Asseng, S., Ewert, F., 2024. Mechanisms and modelling approaches for excessive rainfall stress on cereals: Waterlogging, submergence, lodging, pests and diseases. Agric. For. Meteor. 344, 109819. https://doi.org/10.1016/j.agrformet.2023.109819.
Kong, L., Xie, Y., Hu, L., Feng, B., Li, S., 2016. Remobilization of vegetative nitrogen to developing grain in wheat (*Triticum aestivum* L. Field Crop. Res. 196, 134–144.
Kundel, D., Meyer, S., Birkhofer, H., Fliessbach, A., Mäder, P., Scheu, S., van Kleunen, M., Birkhofer, K., 2018. Design and manual to construct rainout-shelters for climate change experiments in agroecosystems. Front. Environ. Sci. 6. https://doi.org/10.3389/fenvs.2018.00014.
Ladha, J.K., Pathak, H., Krupnik, T.J., Six, J., van Kessel, C., 2005. Efficiency of fertilizer nitrogen in cereal production: retrospects and prospects. Adv. Agron. 87, 85–156. https://doi.org/10.1016/S0065-2113(05)87003-8.
Ladha, J.K., Tirol-Padre, A., Reddy, C.K., Cassman, K.G., Verma, S., Powlson, D.S., van Kessel, C., Richter, D., de, B., Chakraborty, D., Pathak, H., 2016. Global nitrogen budgets in cereals: A 50-year assessment for maize, rice and wheat production systems. Sci. Rep. 6, 19355. https://doi.org/10.1038/srep19355.
Lehmann, N., Finger, R., Klein, T., Calanca, P., Walter, A., 2013. Adapting crop management practices to climate change: Modeling optimal solutions at the field scale. Agric. Syst. 117, 55–65.
Levy, L., Schwaerzel, R., Kleijer, G., 2007. Influence de la fumure azotée sur la qualité des céréales panifiables. Rev. Suisse Agric. 39 (5), 255–260.
Liu, E.K., Mei, X.R., Yan, C.R., Gong, D.Z., Zhang, Y.Q., 2016. Effects of water stress on photosynthetic characteristics, dry matter translocation and WUE in two winter wheat genotypes. Agric. Water Manag 167, 75–85. https://doi.org/10.1016/j.agwat.2015.12.026.
Liu, H., Pequeno, D.N.L., Hernández-Ochoa, I.M., Krupnik, T.J., Sonder, K., Xiong, W., Xu, Y. A consistent calibration across three wheat models to simulate wheat yield and phenology in China., 2020. Ecological Modelling 430, 109132, ISSN 0304-3800. https://doi.org/10.1016/j.ecolmodel.2020.109132.
Martre, P., Dueri, S., Guarin, J.R., Ewert, F., Webber, H., Calderini, D., Molero, G., Reynolds, M., Miralles, D., Garcia, G., Brown, H., George, M., Craigie, R., Cohan, J.-P., Deswarte, J.-C., Slafer, G., Giunta, F., Cammarano, D., Ferrise, R., Gaiser, T., Gao, Y., Hochman, Z., Hoogenboom, G., Hunt, L.A., Kersebaum, K.C., Nendel, C., Padovan, G., Ruane, A.C., Srivastava, A.K., Stella, T., Supit, I., Thorburn, P., Wang, E., Wolf, J., Zhao, C., Zhao, Z., Asseng, S., 2024. Global needs for nitrogen fertilizer to improve wheat yield under climate change. Nat. Plants 10, 1081–1090. https://doi.org/10.1038/s41477-024-01739-3.
Matthews, R.B., Rivington, M., Muhammed, S., Newton, A.C., Hallett, P.D., 2013. Adapting crops and cropping systems to future climates to ensure food security: the role of crop modelling. Glob. Food Secur. 2 (1), 24–28.
Moghaddam, H., Oveisi, M., Mehr, M.K., Bazrafshan, J., Naeimi, M.H., Kaleibar, B.P., Müller-Schärer, H., 2023. Earlier sowing combined with nitrogen fertilization to adapt to climate change effects on yield of winter wheat in arid environments: results from a field and modeling study. Eur. J. Agron. 146, 126825. https://doi.org/10.1016/j.eja.2023.126825.
Mohammadi, R., 2024. Effects of post-flowering drought and supplemental irrigation on grain yield and agro-phenological traits in durum wheat. Eur. J. Agron. 156, 127180. https://doi.org/10.1016/j.eja.2024.127180.
Monteith, J., 1996. The quest balance in crop model. Agron. J. 88, 695–697.
Nguyen, T.H., Langensiepen, M., Gaiser, T., Webber, H., Ahrends, H., Hueging, H., Ewert, F., 2022. Responses of winter wheat and maize to varying soil moisture: from leaf to canopy. Agric. For. Meteor. 314, 108803. https://doi.org/10.1016/j.agrformet.2021.108803.
Nóia Júnior, R., de, S., Deswarte, J.-C., Cohan, J.-P., Martre, P., van der Velde, M., Lecerf, R., Webber, H., Ewert, F., Ruane, A.C., Slafer, G.A., Asseng, S., 2023b. The extreme 2016 wheat yield failure in France. Glob. Chang. Biol. 29, 3130–3146. https://doi.org/10.1111/gcb.16662.
Nóia Júnior, R. de S., Asseng, S., García-Vila, M., Liu, K., Stocca, V., dos Santos Vianna, M., Weber, T.K.D., Zhao, J., Palosuo, T., Harrison, M.T., 2023a. A call to action for global research on the implications of waterlogging for wheat growth and yield. Agric. Water Manag 284, 108334. https://doi.org/10.1016/j.agwat.2023.108334.
Onyemaobi, I., Liu, H., Siddique, K.H.M., Yan, G., 2017. Both male and female malfunction contributes to yield reduction under water stress during meiosis in bread wheat. Front. Plant Sci. 7. https://doi.org/10.3389/fpls.2016.02071.
Pedro, A., Savin, R., Parry, M.A.J., Slafer, G.A., 2012. Selection for high grain number per unit stem length through four generations from mutants in a durum wheat population to increase yields of individual plants and crops. Field Crop. Res. 12, 59–70. https://doi.org/10.1016/j.fcr.2012.01.016.
Peña-Bautista, R.J., Hernandez-Espinosa, N., Jones, J.M., Guzman, C., Braun, H.J., 2017. CIMMYT series on carbohydrates, wheat, grains, and health wheat-based foods: their global and regional importance in the food supply, nutrition, and health. Cereal Foods World 62, 231–249.
Pequeno, D.N.L., Hernández-Ochoa, I.M., Reynolds, M., Sonder, K., MoleroMilan, A., Robertson, R.D., Lopes, M.S., Xiong, W., Kropff, M., Asseng, S., 2021. Climate impact and adaptation to heat and drought stress of regional and global wheat production. Environ. Res. Lett. 16, 054070. https://doi.org/10.1088/1748-9326/abd970.
Qaseem, M.F., Qureshi, R., Shaheen, H., 2019. Effects of pre-anthesis drought, heat and their combination on the growth, yield and physiology of diverse wheat (*Triticum aestivum* L.) genotypes varying in sensitivity to heat and drought stress. Sci. Rep. 9, 6955. https://doi.org/10.1038/s41598-019-43477-z.
Rahman, M.Z., Islam, M.R., Islam, M.T., Karim, M.A., 2014. Dry matter accumulation, leaf area index and yield responses of wheat under different levels of nitrogen. Bangladesh J. Agric. 7 (1), 27–32.
Ritchie, J.T., Singh, U., Godwin, D.C., Bowen, W.T., 1998. Cereal growth, development and yield. Understanding options for agricultural production. Kluwer Acad. Publ. Dordr. Neth. 79–98.
Ru, C., Wang, K., Hu, X., Chen, D., Wang, W., Yang, H., 2023. Nitrogen modulates the effects of heat, drought, and combined stresses on photosynthesis, antioxidant capacity, cell osmoregulation, and grain yield in winter Wheat. J. Plant Growth Regul. 42, 1681–1703. https://doi.org/10.1007/s00344-022-10650-0.
Schulz, R., Makary, T., Hubert, S., Hartung, K., Gruber, S., Donath, S., Dohler, J., Weis, K., Ehrhart, E., Claupein, W., Piepho, H., Pekrun, C., Muller, T., 2015. Is it necessary to split nitrogen fertilization for winter wheat? On-farm research on Luvisols in South-West Germany. J. Agric. Sci. 153, 575–587. https://doi.org/10.1017/S0021859614000288.
Shelia, V., Asseng, S., Porter, C., Hoogenboom, G., 2019. Simulation of a perched water table with impact on wheat crop growth, in: Agricultural and Biological Engineering University of Florida. Gainesville.
Shoukat, M.R., Wang, J., Habib-ur-Rahman, M., Hui, X., Hoogenboom, G., Yan, H., 2024. Adaptation strategies for winter wheat production at farmer fields under a changing climate: Employing crop and multiple global climate models. Agric. Syst. 220, 104066. https://doi.org/10.1016/j.agsy.2024.104066.
Sinaj, S., Charles, R., Baux, A., Dupuis, B., Hiltbrunner, J., Levy Häner, L., Pellet, D., Blanchet, G., Jeangros, B., 2017. Düngung von Ackerkulturen: Grundlagen für die Düngung landwirtschaftlicher Kulturen in der Schweiz (GRUD) Agrarforschung Schweiz, 8, (6): Spezialpublikation, 1–46 / Fertilisation des grandes cultures: Principes de fertilisation des cultures agricoles en Suisse (PRIF) Recherche Agronomique Suisse, 8, (6): Publication spéciale, 1–46 / Concimazione delle colture erbacee da pieno campo: Principi di concimazione delle colture agricole in Svizerra (PRIC) Recherche Agronomique Suisse, 8, (6), 2017, Pubblicazione speciale, 1–45.
Steduto, P., Hsiao, T.C., Fereres, E., Raes, D., 2012. Crop yield response to water - FAO Irrigation and Drainage Paper 66. FAO Rome.
Swiss granum, 2020. Übernahmebedingungen Brot- und Futtergetreide, Eiweisspflanzen.
Thompson, R.B., Tremblay, N., Fink, M., Gallardo, M., Padilla, F.M., 2017. Tools and Strategies for Sustainable Nitrogen Fertilisation of Vegetable Crops. In: Tei, F., Nicola, S., Benincasa, P. (Eds.), Advances in Olericulture, Advances in Research on Fertilization Management of Vegetable Crops. Springer, Cham. https://doi.org/10.1007/978-3-319-53626-2_2.
Touzy, G., Rincent, R., Bogard, M., Lafarge, S., Dubreuil, P., Mini, A., Deswarte, J.-C., Beauchêne, K., Le Gouis, J., Praud, S., 2019. Using environmental clustering to identify specific drought tolerance QTLs in bread wheat (*T. aestivum* L.). Theor. Appl. Genet 132, 2859–2880. https://doi.org/10.1007/s00122-019-03393-2.
Triboi, E., Triboi-Blondel, A.-M., 2002. Productivity and grain or seed composition: a new approach to an old problem. Eur. J. Agron. 16, 163–186. https://doi.org/10.1016/S1161-0301(01)00146-0.
Wang, B., Li, R., Wan, Y., Li, Y., Cai, W., Guo, C., Qin, X., Song, C., Wilkes, A., 2021. Air warming and CO_2 enrichment cause more ammonia volatilization from rice paddies: An OTC field study. Sci. Total Environ. 752, 142071. https://doi.org/10.1016/j.scitotenv.2020.142071.
Wang, E., Martre, P., Zhao, Z., Ewert, F., Maiorano, A., Rötter, R.P., Kimball, B.A., Ottman, M.J., Wall, G.W., White, J.W., Reynolds, M.P., Alderman, P.D., Aggarwal, P. K., Anothai, J., Basso, B., Biernath, C., Cammarano, D., Challinor, A.J., De Sanctis, G., Doltra, J., Dumont, B., Fereres, E., Garcia-Vila, M., Gayler, S., Hoogenboom, G., Hunt, L.A., Izaurralde, R.C., Jabloun, M., Jones, C.D., Kersebaum, K.C., Koehler, A.-K., Liu, L., Müller, C., Kumar, S.N., Nendel, C., O'Leary, G., Olesen, J.E., Palosuo, T., Priesack, E., Rezaei, E.E., Ripoche, D., Ruane, A.C., Semenov, M.A., Shcherbak, I., Stöckle, C., Stratonovitch, P., Streck, T., Supit, I., Tao, F., Thorburn, P., Waha, K., Wallach, D., Wang, Z., Wolf, J., Zhu, Y., Asseng, S., 2017. The uncertainty of crop yield projections is reduced by improved temperature response functions. Nat. Plants 3 (8), 17102. https://doi.org/10.1038/nplants.2017.102.
Wang, Y., Peng, Y., Lin, J., Wang, L., Jia, Z., Zhang, R., 2023. Optimal nitrogen management to achieve high wheat grain yield, grain protein content, and water productivity: a meta-analysis. Agric. Water Manag 290, 108587. https://doi.org/10.1016/j.agwat.2023.108587.
Webber, H., Ewert, F., Olesen, J.E., Müller, C., Fronzek, S., Ruane, A.C., Bourgault, M., Martre, P., Ababaei, B., Bindi, M., Ferrise, R., Finger, R., Fodor, N., Gabaldón-Leal, C., Gaiser, T., Jabloun, M., Kersebaum, K.-C., Lizaso, J.I., Lorite, I.J., Manceau, L., Moriondo, M., Nendel, C., Rodríguez, A., Ruiz-Ramos, M., Semenov, M. A., Siebert, S., Stella, T., Stratonovitch, P., Trombi, G., Wallach, D., 2018. Diverging importance of drought stress for maize and winter wheat in Europe. Nat. Commun. 9, 4249. https://doi.org/10.1038/s41467-018-06525-2.
Willmott, C.J., 1982. Some comments on the evaluation of model performance. Bull. Am. Meteorol. Soc. 63 (11), 1309–1313.
WRBSR (World Reference Base for Soil Resources), 2014. International soil classification system for naming soils and creating legends for soil maps. In: World Soil Resources Reports no, 106. FAO, Rome, Italy.

Xiong, X., Chang, L., Khalid, M., Zhang, J., Huang, D., 2018. alleviation of drought stress by nitrogen application in Brassica campestris ssp. Chinensis L. Agron 8, 66. https://doi.org/10.3390/agronomy8050066.

Ye, Z., Qiu, X., Chen, J., Cammarano, D., Ge, Z., Ruane, A.C., Liu, L., Tang, L., Cao, W., Liu, B., Zhu, Y., 2020. Impacts of 1.5 °C and 2.0 °C global warming above pre-industrial on potential winter wheat production of China. Eur. J. Agron. 120, 126149. https://doi.org/10.1016/j.eja.2020.126149.

Zandalinas, S.I., Mittler, R., Balfagón, D., Arbona, V., Gómez-Cadenas, A., 2018. Plant adaptations to the combination of drought and high temperatures. Physiol. Plant 162 (1), 2–12. https://doi.org/10.1111/ppl.12540.

Zhang, X., Chen, S., Sun, H., Pei, D., Wang, Y., 2008. Dry matter, harvest index, grain yield and water use efficiency as affected by water supply in winter wheat. Irrig. Sci. 27, 1–10. https://doi.org/10.1007/s00271-008-0131-2.

Zheng, Y., He, C., Guo, L., Hao, L., Cheng, D., Li, F., Peng, Z., Xu, M., 2020. Soil water status triggers CO_2 fertilization effect on the growth of winter wheat (Triticum aestivum). Agric. For. Meteor. 291, 108097. https://doi.org/10.1016/j.agrformet.2020.108097.

Zörb, C., Ludewig, U., Hawkesford, M.J., 2018. Perspective on wheat yield and quality with reduced nitrogen supply. Trends Plant Sci. 23, 1029–1037. https://doi.org/10.1016/j.tplants.2018.08.012.